Chapter 3
Electrical Discharge Micro-hole Machining Process of Ti–6Al–4V: Improvement of Accuracy and Performance

Golam Kibria, I. Shivakoti, B.B. Pradhan and B. Bhattacharyya

Abstract Micro-electrical discharge machining (Micro-EDM) has become one of the promising micromachining processes utilizing which high accurate intricate micro-features can be machined efficiently in shop floor. In this chapter, an overview of micro-EDM process and its capabilities is presented for obtaining different desired shape/profile utilizing various machining techniques. The chapter also deals with differences between EDM and micro-EDM, details of system components and micro-EDM process parameters. The significant performance characteristics of micro-EDM process are also discussed. For improving the machining rate as well as for producing high accurate micro-features in different engineering materials, experimental investigation of micro-hole drilling process on Ti–6Al–4V material is carried out implementing several innovative machining strategies such as comparative study of employing kerosene and de-ionized water as dielectrics, the effects of mixing of boron carbide additive in kerosene and de-ionized water, effects of polarity changing between the electrode and effects of rotating the micro-tool. Detailed parametric analysis is carried out to explore the effects of process parameters utilizing these novel machining strategies. Optical and SEM micrographs taken at different parametric combinations have also been analyzed.

G. Kibria (✉)
Mechanical Engineering Department, Aliah University, Kolkata 700156, India
e-mail: prince_me16@rediffmail.com

I. Shivakoti · B.B. Pradhan
Mechanical Engineering Department, Sikkim Manipal Institute of Technology, Sikkim 737132, India
e-mail: ishwar.siwa@gmail.com

B.B. Pradhan
e-mail: bbpradhan1@rediffmail.com

B. Bhattacharyya
Production Engineering Department, Jadavpur University, Kolkata 700032, India
e-mail: bb13@rediffmail.com

G. Kibria et al. (eds.), *Non-traditional Micromachining Processes*,
Materials Forming, Machining and Tribology,
DOI 10.1007/978-3-319-52009-4_3

3.1 Introduction

In the last several years, it has been seen that the demand of micromachining technologies has increased in every shop floor and in wide range of industry segment from biomedical appliances to aerospace products or parts and automotive world. Technocrats and manufacturing engineers are always seeking the challenges to develop new micro manufacturing techniques to manufacture products from hard-to-machine materials to meet the requirement of product miniaturization considering numerous technical challenges. Therefore, to support the growth of product miniaturization and to manufacture micro components effectively and efficiently, it is the responsibility of manufacturing researchers to develop appropriate micro manufacturing processes which have the ability to meet the above-mentioned challenges [1]. Micro-electrical discharge machining (μ-EDM) is an cost-effective and widely utilized micromachining process for machining materials which are difficult-to-machine in conventional methods. The inaccuracies due to vibration of tool or workpiece can be eliminated in this process because the machining method is non-contact and thermo-electric type [2]. Material erosion using controlled spark discharges was first reported by B.R. and N.I. Lazarenko in 1940s in the Union Soviet Socialist Republics (USSR). After that, significant progress and developments of EDM technologies has been carried out by researchers worldwide to control the discharge phenomena, develop reliable machine tools, implementing adaptive control mechanism, employ computer numerical control (CNC), increase accuracy of geometrical features, high precision micro-tool fabrication, tool wear compensations, etc.

3.2 Brief Overview of EDM and Micro-EDM

In Electrical Discharge Machining (EDM) process, controlled spatially and temporally separated pulsed discharges is created between the tool and workpiece in a very narrow inter electrode gap (IEG). The material removal from electrically conductive material is irrespective of the thermal, physical, chemical and mechanical properties [3]. During discharge between the tool tip and workpiece surface, the machining zone must be immerged in dielectric fluid namely kerosene, EDM oil, de-ionized water and paraffin oil etc. The schematic view of basic EDM principle is depicted in Fig. 3.1. The discharge is produced at the location of IEG where there is smallest gap underneath the tool tip surface. The succession phenomena which occur during a typical discharge between the electrodes i.e. at IEG is shown in Fig. 3.2. When a pulsed DC is applied between two electrodes kept at very small electrode gap, strong electrical field is generated. Due to the electromagnetic field, the microscopic contaminants suspended in the dielectric fluid

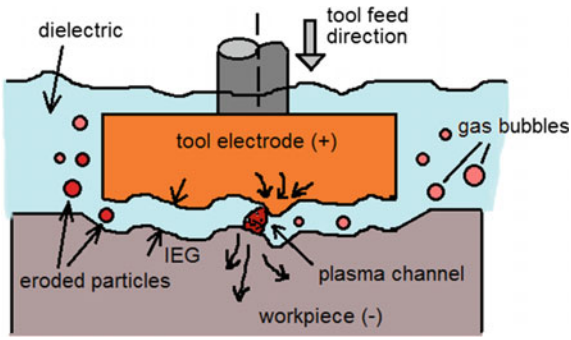

Fig. 3.1 Schematic representation of EDM process

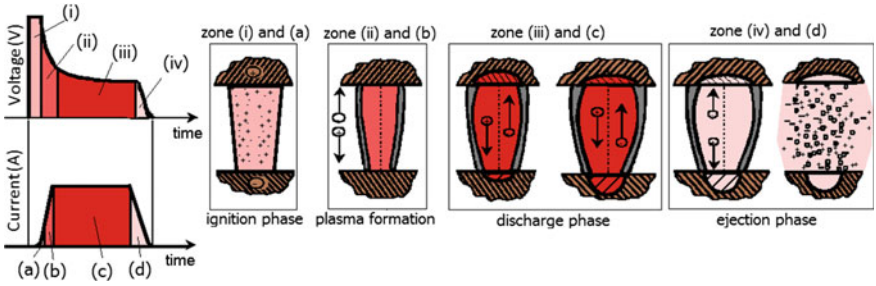

Fig. 3.2 Representation of typical voltage and current trends with sequential phenomena occurring due to single discharge

initiate to drift and they align at the strongest point of the field. These contaminants along with other particles construct the conductive bridge across the IEG, typical spark gap distance varies from 10 to 100 μm. As voltage between the electrode and workpiece increases at the beginning of the pulse, the surface temperature of the workpiece material increases. Some amount of the dielectric fluid and charged particles of the conductive bridge vaporizes and ionizes thereby forming a plasma channel. When the potential difference across the spark gap sharply falls, voltage breakdown occurs. At this time, the plasma channel starts to conduct the applied current whose magnitude rises instantaneously. The abrupt increase in current creates instantaneous increase in localized temperature and pressure in the plasma channel. During discharge between the tool and workpiece, when the local temperature rises beyond the melting point of work material, material melted and vaporized at the location of discharge and small tiny debri particles are ejected out from material's surface creating several number of craters [4]. The gaseous bubbles in the plasma channel expand outward radially from the point of its origin.

At the end of the discharge, the supply of electrical pulse is terminated. This sudden termination of the pulsed power results in collapse of plasma channel and consequently the vapour bubble under the influence of pressure imposed by dielectric fluid from surrounding. The violent in rush of relatively cool dielectric fluid creates an explosive expulsion of molten materials both from the tool electrode. Due to discharge, small amount of material from tool electrode is also removed creating geometrical inaccuracies of shape and size of tool. The debri particles are removed from the machining zone by fresh dielectric fluid supplied by the flushing jet.

The principle of material removal phenomena from workpiece in micro-EDM is same as EDM process. However, the differences such as utilizing micro sized tool, the amount of discharge energy and the X-Y-Z axes resolution make the micro-EDM process more precise and reliable and capable of micro features generation [1, 5]. In micro-EDM, very high frequency pulses (>200 Hz), small discharge energies (10^{-6}–10^{-7} J) and applied potential difference (40–100 V) between the electrodes are applied to achieve high accuracy features and surface finish (roughness as much as 0.1 μm) [6]. Utilizing improved pulse generator and precise servo feed system, the micro-tool electrode can be moved at micron rate to maintain the required IEG and also to retract the micro tool if the servo feed senses any short-circuit between the electrodes. In micro-EDM, the type of dielectric flushing and the value of flushing pressure are important parameters as during machining, micro-tool may vibrates at high dielectric pressure and deteriorate the accuracy of micro features to be produced.

Micro-EDM is not only the scaled down version of EDM process, but also there are significant differences of these two processes in terms of tool electrode type, shape and dimensions, range of discharge energy, resolution of moving axis, inter electrode gap control, type of dielectric flushing for debris removal, etc. The radius of plasma channel in micro-EDM is comparable with tool dimension as micro-EDM uses micro-tool electrode. However, in EDM, size of plasma channel is much less compared to tool size [7]. As in micro-EDM, material removal per discharge (unit removal, UR) should be less; therefore, the applied discharge energy is limited. On the other hand, in EDM, unit removal is much higher. Further, to avoid the micro-tool to be rupture or burnt due to excessive discharge energy, the maximum applied energy in micro-EDM is limited. As in micro-EDM, small sized (in micron dimensions) tool electrode is used and it has low electrode stiffness, thus, during micro machining operation in micro-EDM, micro-tool may vibrate due to flushing pressure and geometrical accuracy of micro features to be produced is deteriorated. Therefore, the range of dielectric flushing pressure is kept in lower settings. This problem is absent in EDM process. Further, in micro-EDM, the amount of thermal load on micro-sized tool electrode is high and thus, the amount of tool wear also high compared to conventional EDM. Thus, various tool wear compensation strategies are considered for generating precise and accurate micro features. Due to very low IEG in micro-EDM, short circuiting occurs frequently,

which renders machined surface uneven. Moreover, when the debris are ejecting out from work material, secondary sparking occurs and geometry of micro-tool get degenerated. These drawbacks are very less in conventional EDM.

3.3 Micro-EDM System Details

The micro EDM system typically consist of several sub-components such as servo system, control unit, positioning system, dielectric circulating unit and the working chamber. Figure 3.3 shows the schematic diagram of micro EDM system with sub-systems. The servo system guides the micro electrode during the machining and the feed movement of micro-electrode is controlled by the servo control unit. The workpiece is firmly held in the working table and the positioning system control the movement of work chamber in the X and Y axis. The constant feed of the micro-tool is given by servo feed mechanism in Z axis direction. The dielectric circulating system is another important component in micro-EDM in which continuous flow of fresh dielectric fluid is supplied to the machining chamber. The servo control unit is one of the essential components of micro EDM as it controls the movement of micro-tool and also it maintains the inter-electrode gap between the micro-tool and the workpiece in micron range. In order to generate dimensional accurate features, it is very important to keep constant inter electrode gap between the electrodes [8]. The dielectric system serves an important role in micro-EDM as the dielectric possesses a crucial role during machining. The dielectric tank contains a dielectric which is pumped to the machining chamber. The pressure regulator controls the flushing pressure of the dielectric jet onto the machining chamber. The dielectric is continuously circulated for efficient machining and the used dielectric is passed through the micro filters which captured the debris particle generated during machining. The dielectric jet removes the debris from work material and also it serves as insulation between the micro tool and the work material. Further, the

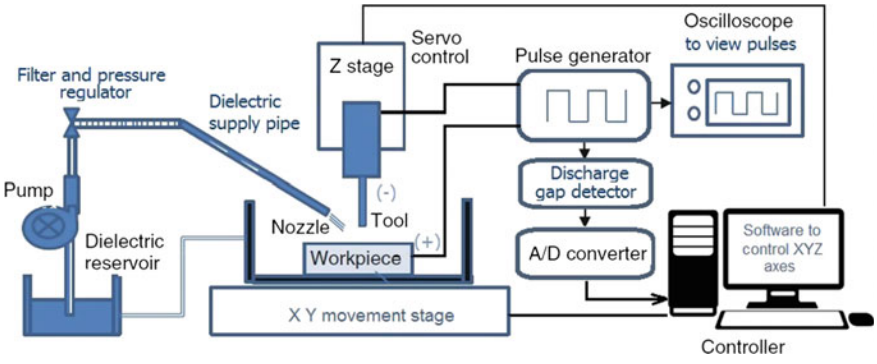

Fig. 3.3 Schematic diagram of a typical micro-EDM system showing different sub-systems

dielectric is required for the ionization and act as a medium to cool the micro-tool and the workpiece.

3.4 Pulse Generators for Micro-EDM

The series of pulse has been generated for micro EDM with the help of pulse generator. The various type of pulse generator has been used for producing series of pulse for micro-EDM process. In RC type capacitor, the charging time is more and due to this, it cannot produce high frequency pulses and it also produces thermal damage of the wok material. Sometimes, discharge current flows through the previous plasma channel without recharging the series of capacitors [9]. Since the capacitor is absent in the transistor type pulse generator as a result high discharge frequency pulses is produced which enhances the material removal rate. Moreover, the transistor type pulse generator is controlled easily as compared to RC type generator. The transistor type pulse generator cannot be used when nanoseconds pulses are required for machining as it is not capable of producing nanoseconds pulses. To reduce the delay time of transistor-type pulse generator, the transistor-type isopulse generator was developed and successfully employed for micro-EDM operation [10]. For rough and semi finish machining, a field effect transistor is used to cut off the discharge current. Instead of observing the gap voltage, the pulse current is observed for detecting the discharge. As the current sensor provide an output less than 5 V and also it acts as input to pulse control circuit, it eliminates the voltage attenuation circuit. In this way, the delay time is shortened to significant amount and ultimately, about 80 ns pulse duration was achieved. As in RC-type pulse generator, stray capacitance determines the minimum discharge energy per pulse, therefore, it act as the limitation for generating micro-features on workpiece [11]. Due to difficulty in eliminating the stray capacitance, crater diameter less than 2 μm cannot be achieved [12]. To avoid these problems, a capacity coupling based pulse generator was developed. In this generator, the effect of the stray capacitance can be eliminated as electric feeding is done without touching the micro-tool electrode. Thus, discharge crater dimension of nanometer domain is realized.

3.5 Control Parameters of Micro-EDM

The micro EDM process parameters have significant effect on various process performances. The proper selection of control parameters results in better machining performance. Figure 3.4 shows the fish-bone diagram showing all process parameters related to machining parameters, work material, tool-electrode, polarity, flushing pressure, etc. The micro EDM control parameters are categorized as follows: (a) electrical (b) non-electrical and (c) gap and motion control parameters. Brief discussions on these process parameters are given hereunder.

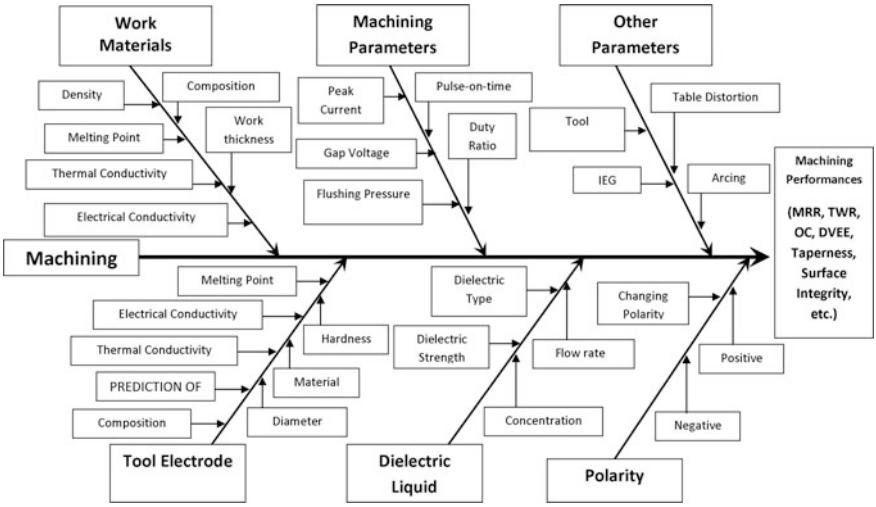

Fig. 3.4 Representation of process parameters in micro-EDM using fish-bone structure

3.5.1 Electrical Process Parameters

(a) **Discharge energy**: In micro-EDM, the most significant process parameter is discharge energy. This parameter is a collection of other operating parameters which are related to the energy of the discharge created between the electrodes at inter electrode gap. For different type of pulse generator, the calculation for discharge energy is different. The material removal rate is directly related to discharge energy during micro-EDM operation. On the contrary, tool wear ratio also increases, which deteriorate the surface finish and accuracy of micro features generated.

(b) **Gap voltage**: Gap voltage is the voltage in the gap between the two electrodes. The total energy of the spark is determined by applied voltage. Depending upon the setting of voltage, the IEG is set by servo control. Larger value of IEG improves the flushing of debris from machining zone and makes the next discharge stable and ultimately improves material removal rate. However, the surface finish deteriorated due to large size of crater dimension at high voltage condition. The voltage of IEG at which discharge occurs between the micro tool and workpiece is known as discharge voltage. The discharge voltage mainly depends upon the breakdown strength of the dielectric and IEG.

(c) **Peak current**: The average current is the average of amperage in spark gap measured over a complete cycle. This is read on the ammeter during the process. The theoretical average current can be measured by multiplying the duty cycle and the peak current i.e. maximum current available for each pulse from the power supply. The amount of energy/power which is used for discharge is mainly determined by peak current. Higher value to peak current signifies better

machining efficiency in terms of material removal rate. At the same time, the surface finish is deteriorated and tool wear ratio increases.

(d) **Duty factor**: Duty factor is the ratio between the pulse duration to the total cycle time. Mathematically, it is evaluated by using Eq. (3.1)

$$Duty\ factor\ (DF)\% = \frac{Pulse\ duration}{Cycle\ time} \times 100\% \tag{3.1}$$

If the duty factor is high, the flushing time is very less and this might lead to the short circuit condition and a small duty factor indicates a high pulse off time and low machining rate.

(e) **Pulse duration**: Pulse duration or pulse-on-time is the time interval in which the applied current is flowing through the IEG of two electrodes. In this time period, breakdown of dielectric occurred and removal of material from work-piece surface takes place. Large value of pulse duration means higher material removal rate. Broader and deeper craters are achieved at longer the pulse duration setting and consequently, rough machined surface is attained. On the contrary, smaller craters which are obtained at low value of pulse duration provides smoother surface finish.

(f) **Polarity**: Polarity refers to the electrical conditions determining the direction of the current flow relative to the electrode. The polarity condition of electrodes is of two type, (i) straight polarity and (ii) reverse polarity. Straight polarity is that condition when the micro tool is connected to cathode (−), whereas, reverse polarity is that condition in which tool electrode is connected to anode (+) and workpiece to cathode (−). For achieving high material removal rate from workpiece, tool electrode is used as cathode and workpiece as anode. Depending on the application, some electrode/work material combinations provide better results when the polarity is changed. Generally for graphite electrode, a positive polarity gives better wear condition and negative polarity gives better machining speed.

(g) **Pulse frequency**: It is the measure of number of cycle per second. Larger value of pulse frequency decreases the pulse duration which results in minimum thermal damage in the work piece during machining. However, at high value of pulse frequency, the surface finish of the machined surface is improved.

3.5.2 Nonelectrical Process Parameters

(a) **Micro-tool electrode**: Tool electrode is an important part for achieving effective and efficient machining condition. The thermal properties of tool electrode material play a significant role during micro-EDM as it is a thermal

process. Materials of higher melting, boiling points and heat conductivity are used to fabricate the micro-tool for micro-EDM process [13]. There are several criteria to choose proper tool electrode materials such as (i) machinability, (ii) electrical and thermal conductivity, (iii) density, (iv) Hardness and toughness, (v) cost and availability, (vi) material removal rate and wear ratio, etc.

(b) **Work materials**: The micro EDM can only machine electrically conductive materials. Moreover, for efficient machining, the thermal properties of the material such as thermal conductivity, specific heat, melting point are the important aspects need to be considered while selecting the work piece material [14].

(c) **Dielectric fluids**: The dielectric fluid has significant role during micro-EDM possess as without it, it is no longer possible to generate efficient discharge between the micro-tool tip and workpiece surface. The quality of surface finish and geometrical accuracy of machined parts depend on several properties of dielectric such as viscosity, dielectric strength, cooling capability, chemical compositions, etc. For safe machining operation and stable sparking condition, the dielectric strength and flash point temperature of the dielectric fluid should be higher. Furthermore, low value of viscosity and specific gravity are another two desirable properties of dielectric fluid. These properties significantly affect the machining efficiency and consequently improves material removal rate, lowers tool wear rate and enhances the surface finish of machined features.

3.5.3 Gap Control and Motion Parameters

Electrode rotation: The rotation of micro-tool about its axis during the micro-EDM enhances the machining performance as the rotation of micro-tool enhances the flushing action of the debris formed during micro-EDM at inter electrode gap. Due to rotation of micro-tool, a tangential force is produced at small IEG and this leads to effective and efficient discharge by smooth removal of debris through small gap of micro-tool surface and micro-hole wall [15]. Moreover, electrode wear ratio also reduces due to micro-tool rotation.

Tool geometry and shape: The micro-feature generated in the workpiece during micro-EDM is the replication of the micro-tool geometry. Moreover, the geometry of micro-tool has significant effect on tool wear ratio. Depending upon the requirement, the shape of micro-electrode can be circular, rectangular, cylindrical etc. Vibration assisted micro-EDM has significant effect on machining rate and taper during micro-hole drilling [16].

Servo feed: For properly maintaining the discharge gap width and to avoid arcing and short-circuiting between the micro-tool and the workpiece, the servo feed control system play vital role during micro-EDM process. As soon as the value

of average gap voltage approach more than preset threshold voltage of pulse generator, the feed rate of servo increases and compensating the discharge gap between the electrodes and vice versa [3].

Tool and workpiece vibration: The performance of the micro-EDM has been improved by incorporating the vibration of micro-tool or workpiece at certain frequency and amplitude. During vibration of micro-tool or workpiece, the forward and backward motion of tool or workpiece changes the discharge gap and consequently, dielectric fluid pressure in the IEG also changes constantly. When the micro-tool is advancing towards the workpiece, the dielectric fluid is forced out from the machining zone. Then after, when the micro-tool move away from machine zone, fresh dielectric is taken by discharge gap and thus, overall flushing efficiency increases.

Flushing techniques: Dielectric flushing has important role for removing the debris from machining zone and consequently, it enables stable discharge condition by supplying fresh dielectric fluid in the gap. In general, there are mainly two types of flushing, pressure flushing and suction flushing. Depending upon the type of flushing, the amount of flushing pressure is provided. In micro-EDM operation, for effective generation of high aspect ratio micro-features such as micro-holes, jet flushing is more effectively used. In other cases, side flushing is commonly used. If the jet flushing is provided from one direction, there may be chances to accumulate the debris in the downstream, which creates irregular gap width and as a result, accuracy of micro-feature is deteriorated [17]. To avoid this, jet flushing from both side and sweeping type flushing also sometime recommended. In Fig. 3.5, different types of flushing for micro-EDM are illustrated.

Flushing pressure: For quick removal of the debris from the IEG during micro-EDM, it is more important to flush out debris particles from very narrow discharge gap. Higher value of flushing pressure is preferable for effective debris removal, stable machining and high aspect ratio micro-feature generation. However, as stiffness of micro-tool is low, high flushing pressure may deteriorate dimensional accuracy due to micro-tool vibration or deflection.

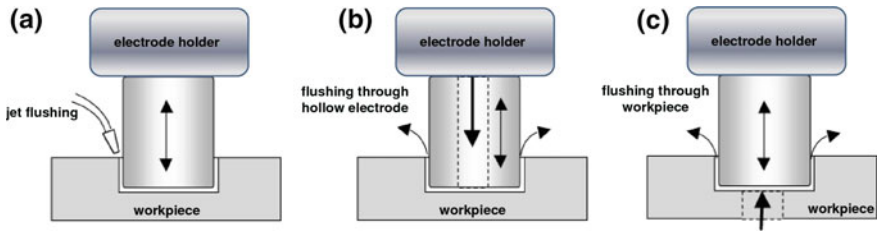

Fig. 3.5 Schematic of **a** jet, **b** flushing through tube electrode and **c** flushing through workpiece in micro-EDM process

3.6 Micro-EDM Performance Measurements

Material removal rate: The amount of material removed from the workpiece per unit time is known as material removal rate (MRR). It is evaluated in terms of volume of material removed from the workpiece or can be evaluated by differentiating the weight of the workpiece taken before and after machining. It is calculated using Eq. (3.2)

$$Material\ removal\ rate\ (MRR) = \frac{Weight\ of\ workpiece\ before\ machining - Weight\ of\ workpiece\ after\ machining}{Machining\ time} \tag{3.2}$$

The higher material removal depicts the increases the productivity and hence, the material removal is always consider to be the higher the better type. Higher MRR can be achieved at high discharge voltage, peak current, pulse duration and duty cycle. However, other desirable process performances such as tool wear ratio, surface finish and dimensional accuracy is also important aspects and taken into account in micro-EDM.

Tool wear rate: The amount of material removed from the micro-tool during machining is known as tool wear rate (TWR). The high electrode wear is not desirable in micro-EDM as it changes the geometry of the tool which reduces quality of the machined surface and inaccurate geometric features are achieved onto the machined surface. The electrode wear is calculated by differentiating the weight of the micro-tool before and after machining and is calculated by Eq. (3.3).

$$Tool\ wear\ rate\ (TWR) = \frac{Weight\ of\ microtool\ before\ machining - Weight\ of\ microtool\ after\ machining}{Machining\ time} \tag{3.3}$$

Surface roughness: Surface roughness of the machined features mainly depends on the crater size (diameter and depth) that is formed by each discharge. In addition, if the dielectric circulation in the discharge gap is not efficient, then some molten material from tool and workpiece resolidifies on the micro-feature surface and makes the surface rough. Thus, effective flushing technique has significant effect on surface finish of the features. Crater dimensions also largely depend on pulse energy of discharge and other process parameters such as peak current, pulse frequency and pulse duration [18]. Required amount of flushing pressure can decrease the roughness of machined surface. Moreover, the properties of material of the micro-tool and the workpiece have considerable effects on surface finish.

Overcut: Overcut is the difference in diameter of the micro-hole at the entrance and the diameter of the tip of the cylindrical shaped micro electrode. It produces inaccuracy in the dimension of the machined features. For micro-hole drilling

process in micro-EDM, overcut is calculated using Eq. (3.4). The overcut occurs mainly due to secondary sparking during material removal from sidewall of the micro-feature surface while the debris try to ejecting out by flushing pressure from the machining zone.

$$Overcut\ (OC) = \frac{Diameter\ of\ entry\ hole - diameter\ of\ microtool\ tip}{2} \tag{3.4}$$

Diameteral variance at entry and exit hole: This performance criterion is related to through micro-hole drilling in micro-EDM. The diameteral variance of entry and exit hole is measured by differentiating the micro-hole diameter at entry and at exit side of from end to end hole on workpiece. During micro-drilling operation of high aspect ratio hole, if the secondary sparking occurs for a long time, then large amount of diameteral difference is realized. Dimeteral variance of entry and exit hole is affected by a number of process parameters such as peak current, pulse duration, duty cycle and flushing pressure.

Circularity: Circularity is the measure of roundness of micro-hole. The circularity of micro-hole is calculated by Eq. (3.5). Due to high flushing pressure or non-uniform discharge condition, the degree of roundness of micro-hole deteriorated and further reduces the circularity of the micro-hole.

$$Circularity = 4\pi \frac{Area\ of\ microhole}{[Perimeter\ of\ microhole]^2} \tag{3.5}$$

Machining time: The time during which the machining is performed in order to produce micro-features on the workpiece. Due to inefficient discharge and various unwanted phenomena, machining time increases for producing particular micro-features on workpiece surface.

3.7 Varieties of Micro-EDM Processes

Depending upon the tool-work configuration and relative motion between the micro-tool and workpiece to be machined, there are several varieties of micro-EDM process. These machining varieties have been developed based upon the requirements of product intricacy and features.

3.7.1 Micro-EDM Drilling

The process in which deep micro-sized hole is generated by EDM process is termed as micro-EDM drilling. In conventional EDM process, both tube and solid electrodes can be used as tool material. However, for micro-EDM, as the geometrical

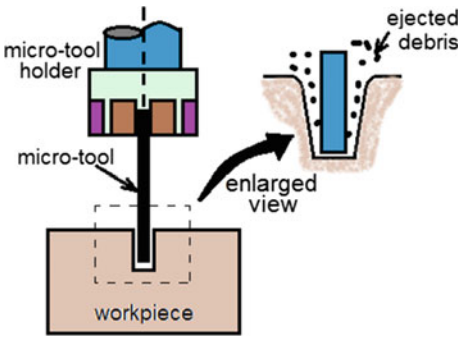

Fig. 3.6 Schematic representation of micro-EDM drilling process with enlarged view of machining zone

dimensions of tool electrode is in micron range, therefore, only solid micro-rods can be used. For efficient removal of eroded particles from the machining zone, it is recommended to employ jet flushing in micro-EDM with low value of flushing pressure to avoid vibration of micro-tool electrode. In Fig. 3.6, the schematic of micro-EDM drilling process is depicted. When the debris particles try to eject out from the IEG, due to secondary sparking between micro-tool and micro-hole walls, material removal is more at entry side of hole and this result in taper in micro-hole geometry. For high precision micro-hole drilling in EDM, sometimes, micro-tool electrode is fabricated in the machine itself by wire-electrical discharge grinding (wire-EDG) process to avoid tool deflection or breakage [19]. Different types of micro-features (irregular, curved, inclined, tapered, etc) can be produced using different alignment of micro-tool as well as tool feed mechanisms. Cooling holes in turbine blades, nozzles for fuel injection system, parts for manufacturing of micro-turbines and surgical instruments are the typical examples of micro-EDM drilling.

3.7.2 Micro Wire-EDM

To cut conductive hard-to-machine materials like Ti-alloy, Ni-alloy, HSS, etc, micro-wire EDM is employed. Micro-wire which is continuously travelling through the upper and lower wire guide, is used here as tool electrode. According to the profile of intricate cut, the machine axes moves in the direction of programmed path and material is removed from workpiece by series of electrical discharges between the micro-wire and workpiece as shown in Fig. 3.7. Since there are additional axes U and V, therefore, taper cutting is possible efficiently by keeping the wire at some angle with vertical by positioning the upper wire guide in respect of lower one [20].

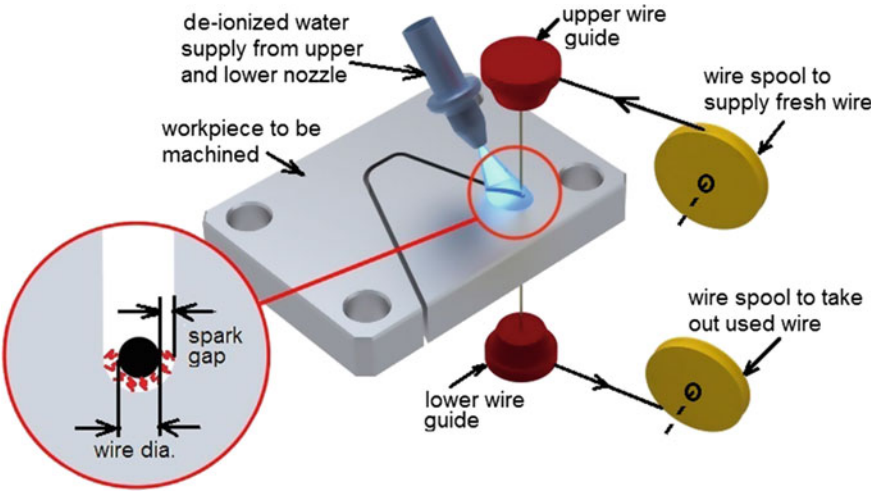

Fig. 3.7 Schematic view of configuration of micro-wire EDM process

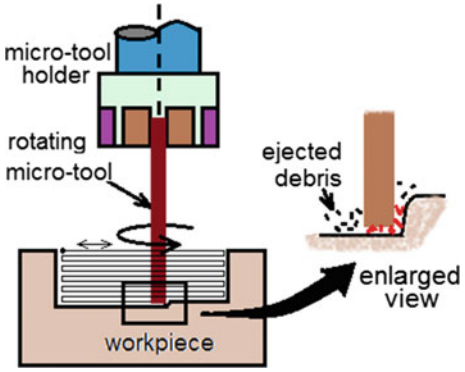

Fig. 3.8 Schematic of micro-EDM milling operation

3.7.3 Micro-EDM Milling

To produce high precision complex geometries, micro-EDM milling is used where the elimination of complex die-sinking tool required for obtaining such profile is possible. The process utilizes cylindrical solid micro-tool electrode to fabricate desired three-dimensional complex structure by scanning the programmed path layer-by-layer using CNC software as shown by schematic representation in Fig. 3.8. Here, the rotation of micro electrode in its axis is a requirement while scanning X-Y planes. Tool length compensation is very much important factor in this process because during layer-by-layer scanning, due to wear of micro-tool, tool length gradually reduced.

3.7.4 Dry and Near-Dry Micro-EDM

In conventional EDM and general micro-EDM processes, mainly hydrocarbon dielectric fluid is used. However, during machining with hydrocarbon oil, harmful vapors are produced which make the machine environment toxic. Thus, to reduce the environmental pollution and also reduce the cost of waste management, dry and near-dry micro-EDM process has been developed. Pure oxygen gas or air is used as dielectric in dry micro-EDM process [21]. However, in near-dry micro-EDM process, mixture of gas and liquid is used as dielectric [22]. The schematic view of dry and near-dry micro-EDM process is depicted in Fig. 3.9. Tube type electrode is used as tool electrode in dry micro-EDM in which air or gas in supplied to the IEG to act as dielectric which ultimately act as cooling medium of micro-tool and workpiece and remove the molten and vaporised material from narrow IEG.

3.7.5 Planetary or Orbital Micro-EDM

In micro-EDM drilling, especially for producing high aspect ratio micro-holes, a common problem is the debris accumulation at machining zone. Due to this, secondary sparking and short-circuiting occur. To avoid this problem, a relative motion (orbital or planetary type) is provided between the micro-tool electrode and workpiece to be machined. The schematic representation of orbital or planetary micro-EDM process is shown in Fig. 3.10. The planetary motion of micro-electrode provides space for dielectric fluid circulation and thus, it helps to reduce the concentration of debris in IEG. It further helps to improve material removal rate, increase the degree of accuracy of micro-structure and reduce tool wear ratio. One of the important benefits of planetary micro-EDM is that in this process, micro-holes of different diameters can be produced by just changing orbital radius and using a single micro-electrode [23].

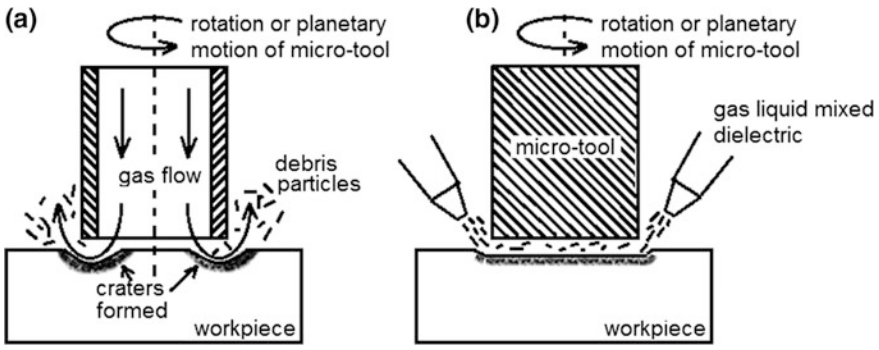

Fig. 3.9 Schematic of **a** dry micro-EDM and **b** near-dry micro-EDM

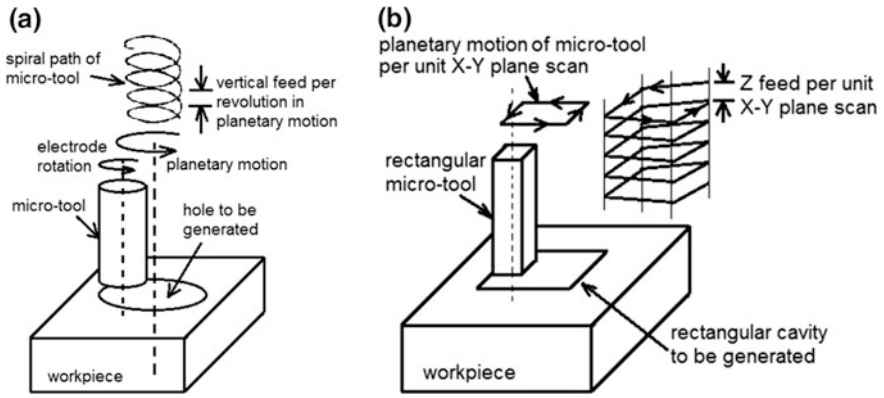

Fig. 3.10 Schematic representation of planetary micro-EDM for generation of **a** circular hole and **b** non-circular hole

3.7.6 Reverse Micro-EDM

For fabrication of high aspect ratio micro-tool electrode, reverse micro-EDM is employed. The process comprises of two steps. In first step, micro-EDM drilling operation is carried out on low thickness material using normal polarity setting. In next step, the material from which high aspect ratio micro-tool electrode is to be fabricated is attached with z axis of machine and already fabricated micro-hole is clamped with machining chamber. The polarity of electrodes is reversed and material erosion takes place from workpiece material as shown in Fig. 3.11. For generating array micro-electrodes on a single material, reverse micro-EDM is an excellent method. The number of micro-electrodes and gap between the electrodes depends upon the number of micro-holes on sacrificial electrode plate.

3.7.7 Micro Electro-discharge Grinding

For fabricating micro-electrode on the machine itself from an electrode material which is larger than required dimensions, micro electro-discharge grinding (micro-EDG) process is employed. The process is classified as (i) block micro-EDG, (ii) moving block micro-EDG, and (iii) micro-wire EDG. In the first type, a sacrificial block (rectangular) with perfectly vertical is used and it should have high degree of wear resistance. If the degree of alignment of the sacrificial block reduces, the geometrical accuracy of fabricated micro-tool by micro-EDG is reduced. Due to wear from sacrificial block, the fabricated micro-electrode diameter is not achieved as straight and wear compensation prediction is difficult to calculate. To overcome this, on-machine dimension measuring instrument and high resolution camera are installed for instantaneous measurement of micro-tool geometries.

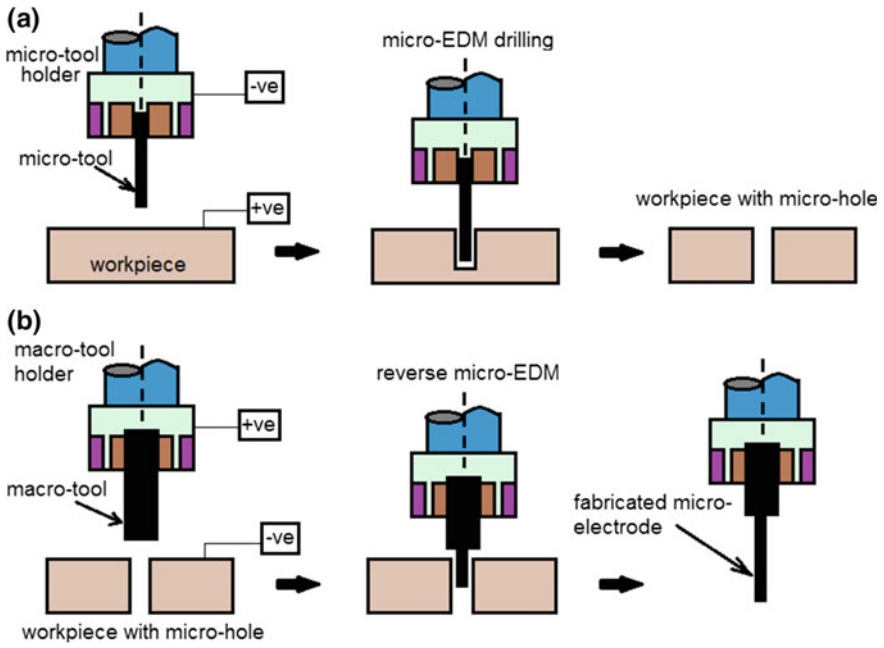

Fig. 3.11 Sequential representation of reverse micro-EDM, **a** micro-hole generation in normal micro-EDM and then **b** fabrication of high aspect ratio micro-electrode using micro-hole

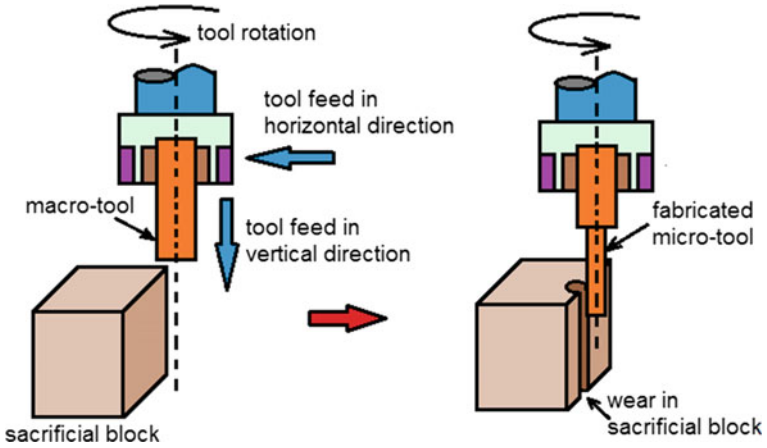

Fig. 3.12 Methodology of stationary block micro-EDG process

The schematic view of block micro-EDG process is shown in Fig. 3.12. During block micro-EDG process, cylindrical material is considered as workpiece and the rectangular block is considered as electrode. During sparking between block surface and rotating workpiece, it is very important factor to apply dielectric jet properly to avoid deflection of material as well as uniformity of micro-tool geometry.

To avoid tapering of micro-electrode in block micro-EDG process, a new and novel micro-EDG process is developed. In moving block micro-EDG, dimensional accurate and high aspect ratio micro-electrode can be fabricated by simply moving the sacrificial block in a direction perpendicular to cylindrical workpiece in addition to rotary and feed movement. In micro-wire EDG process, the workpiece is rotated at vertical axis and a travelling wire is fed towards the rotating workpiece using X and Y axes controller. Due to discharge, material is eroded from travelling wire as well as from workpiece. In Figs. 3.13 and 3.14, the schematic representation of moving block micro-EDG and micro-wire EDG are viewed.

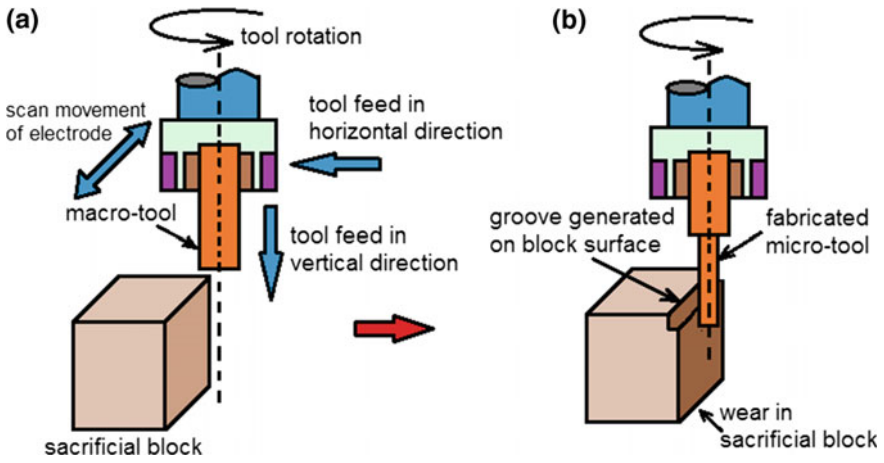

Fig. 3.13 Schematic illustration of moving block micro-EDG, **a** showing the movement of block and macro-tool, **b** fabricated high aspect ratio micro-tool

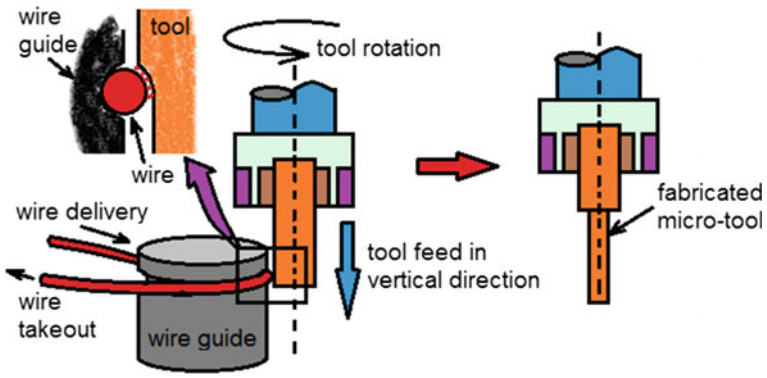

Fig. 3.14 Representation of micro-wire EDG process

3.8 Applications of Titanium and Its Alloys

Titanium alloy was developed in the early 1950s for defence and aeronautic applications due to its very high strength-to-weight ratio. The unique combination of high strength, low weight, and excellent corrosion resistant property of titanium alloy has made it suitable for a wide variety of industrial applications. Its corrosion resistant results from a very thin (−10 nm), stable, continuous oxide layer that regenerates instantaneously if any oxygen or moisture is present. Commercially Pure (CP) Titanium is used primarily for its corrosion resistance. Further titanium alloy can withstand pitting, crevice and cavitations, corrosion, erosion, and stress corrosion cracking in salt water, marine atmospheres, and a broad range of acids, alkalis, and industrial chemicals. This alpha-beta alloy is the workhorse alloy of the titanium industry. The alloy is fully heat-treatable in section sizes up to one inch and is used up to approximately 400 °C. Since it is the most commonly used alloy, over 70% of all alloy grades melted are sub- grade of Ti–6Al–4V. Its uses arc not only confined and concentrated in aerospace engine and airframe components but it is widely uses in major non-aerospace applications in the marine offshore, power generation industries and biomedical applications also. Ti–6Al–4V is the most widely used titanium alloy, accounting for more than half of all titanium tonnage worldwide.

Various excellent properties possessed by titanium super alloys have led to a wide and diversified range of successful applications in medical science as well as in automotive, aerospace, chemical plants, and other precision engineering fields. The wide variety of applications of this exotic material in almost all the precision engineering fields demand the huge need of micro-machining of Ti–6Al–4V. Thus, in order to meet up the huge market demand of micro-products manufactured from Commercially Pure (CP) Titanium and its alloy necessitated the need of micro-machining using micro-EDM technology utilizing different novel machining strategies.

3.9 Brief Background of Machining Ti–6Al–4V in Micro-EDM

In last 15 years, a number of research and development activities have been carried out around the globe for improving the machining performance as well as dimensional accuracy of machined components in micro-EDM process. Moreover, many researchers have utilized various statistical tools for finding out influencing process parameters and optimization of the process for obtaining parametric condition to achieve high performance machining and accurate geometrical features. Micro-hole electro discharge machining has been carried out by Pradhan et al. on Ti–6Al–4V alloy using 500 μm diameter brass micro-electrodes [24]. Four process parameters such as peak current, pulse-on time, flushing pressure and duty ratio

were considered as varying parameters to investigate the process criteria i.e. material removal rate, tool wear rate and overcut. The most influencing process parameters were achieved as peak current and pulse-on time. Flushing pressure and duty factor have no significant effect on material removal rate and tool wear rate. However, overcut of micro-hole generated is mostly affected by peak current and pulse-on-time. Using Response Surface Methodology (RSM) statistical tool, Pradhan and Bhattacharyya investigated the parametric effect on machining performance as well as optimized the process to achieve high MRR, low TWR as well as least overcut during machining of Ti–6Al–4V material [25]. Combined RSM-ANN based mathematic models were developed to correlate machining performances and process parameters. Silicon carbide (SiC) powder additive mixed dielectric was used to investigate and analysis of micro-EDM of Ti–6Al–4V alloy by Ali et al. and the authors concluded that by employing SiC mixed dielectric, material removal rate is enhanced when compared to machining with conventional dielectric [26]. The experimental results revealed that optimization for MRR of 7.31 μg/min is achieved at powder concentration of 24.75 g/L and discharge energy of 56.77 μJ.

Optimization of MRR, TWR and overcut during micro-EDM of Ti–6Al–4V alloy considering voltage, pulse frequency, current and pulse width is achieved by Meena and Azad utilizing combined approach of Taguchi Method and Grey relational analysis (GRA) [27]. Analysis of variance (ANOVA) of the test results have been performed to in order to estimate the predictive accuracy of the developed models and to determine the relative significance of considered process parameters. Hole sinking electrical discharge micromachining (HS-EDMM) process of Ti–6Al–4V thin sheet was carried out by Porwal et al. to develop predictive integrated model (ANN-GRA-PCA) using single hidden layer BPNN [28]. The authors used GRA coupled with PCA hybrid optimization strategy for achieving optimal MRR, TWR and taper of micro-hole at parametric setting of gap voltage of 140 V and capacitance of 100 nF. Experimental investigation and parametric study was carried out by Tiwary et al. during micro-hole machining in micro-EDM of Ti–6Al–4V material based using 1 mm thick titanium alloy material as workpiece and brass electrode of diameter 300 μm as micro-tool on RSM approach considering pulse on time, peak current, gap voltage and flushing pressure as process parameters [29]. Using various surface plots, influences of the process parameters on MRR, TWR, overcut and taper of micro-hole were studied. A combined approach of RSM and fuzzy-TOPSIS method is used to find out optimal parametric combination. The effect of gap voltage, capacitance, rotational speed of electrode and feed rate on MRR during micro-EDM milling operation of Ti–6Al–4V material was investigated by Kuriachen and Mathew [30]. Based on RSM-Box Behnken experimental design, quadratic regression model for MRR was developed and from the test results, it was seen that capacitance and rotational speed of electrode has direct effect on MRR. Study and analysis on the influence of micro-EDM parameters on MRR, TWR, machining time and quality of micro-hole was carried out by Plaza et al. during machining of Ti–6Al–4V [31]. The authors used a new strategy to use helical-shaped micro-tool electrodes. The influences of helix angle and flute depth

of the helical micro-tool on process performances have also been studied. Blind and through micro-holes and micro-slots were machined on brass and Ti–6Al–4V materials by Moses and Jahan [32]. Dimensional accuracy, surface finish, and profile accuracy of holes and slots were measured for analysis. Single through micro-hole, single blind hole, letter H blind, three blind slots and three through slots were machined also. The influence of various process parameters such as pulse-on-time, peak current, gap voltage and flushing pressure on MRR, TWR, overcut and taper of micro-hole during machining of Ti–6Al–4V were studied by Tiwary et al. and empirical models were developed for to correlate the process parameters and machining performances [33]. Multi performance optimization was achieved as MRR of 0.0777 mg/min, TWR of 0.0088 mg/min, OC of 0.0765 mm and taper of 0.0013 at parametric setting of pulse-on-time of 1 μs, peak current of 2.5 A, gap voltage of 50 V, and flushing pressure of 0.20 kgf/cm^2.

Kuriachen and Mathew carried out investigation to machine Ti–6Al–4V with tungsten carbide electrode employing SiC micro particle suspended dielectric during micro-EDM milling operation [34]. The effects of various process parameters such as voltage, capacitance and powder concentration on MRR and TWR was studied. The recommended process parametric setting was powder concentration of 5 g/L, capacitance of 0.1 μF and voltage of 115 V for achieving high material removal and low tool wear rate. Predictive thermal model was developed by B. Kuriachen et al. for simulation of single-spark micro electric discharge machining [35]. The crater geometry and temperature distribution in the workpiece at various process parametric setting were predicted using Gaussian distribution of heat flux, percentage distribution of energy among the workpiece, tool electrode and dielectric. Mathematical model which predicts the radius of the single-spark during micro-EDM process of Ti–6Al–4V was developed by Kuriachen and Mathew [36]. The authors concluded that the spark radius increases proportionally with in capacitance except in the higher energy levels where double sparking phenomenon was observed.

It is observed from the literature review that most of the research investigation and analysis is on investigating the effects of process parameters on machining performances such as MRR, TWR, overcut, surface roughness, etc. Furthermore, optimal parametric combination was also found utilizing several statistical techniques as well as combined approach of different predictive tools for achieving high machining rate, less tool wear rate and good geometrical micro-structures. However, there are many issues which remained unsolved in micro-EDM. Such issues are improving material removal rate, methodology for compensating the micro-tool wear, improving the stability of discharge, improving the accuracy of micro-feature implementing innovative ideas, etc. To solve these important issues and to improve overall micro-EDM efficiency, several new micro-EDM machining strategies have been developed and researchers already started to utilize these innovative strategies during micro-EDM of Ti–6Al–4V material. In the following sections, experimental investigation and analysis of micro-EDM process of Ti–6Al–4V have been carried out extensively utilizing some innovative machining strategies such as ultrasonic vibration assisted micro-ED machining, utilization of

non-hydrocarbon oil as dielectric, reversing the polarity between electrodes, rotating the micro-tool electrode, utilizing powder mixed dielectric fluid, etc.

3.10 Innovative Machining Strategies for Improving Micro-EDM

To achieve effective machining performance of micro-EDM for real time utilization and also for obtaining high productivity with a higher degree of desired accuracy and surface integrity, manufacturer engineers and research scientists are always engaged to develop innovative machining techniques by considering various innovative machining strategies during micro-EDM of various difficult-to-machine materials. In this section, research investigation and analysis in the direction of implementing such novel machining strategies during micro-EDM of Ti–6Al–4V superalloy is discussed.

3.10.1 Ultrasonic Vibration Assisted Micro-EDM

The use of ultrasonic vibration during micro-EDM shows effectiveness for improving machining time as well as geometrical accuracy of fabricated features of micro components. During ultrasonic assisted micro-EDM, micro-tool or dielectric fluid is vibrated ultrasonically. In micro-EDM, the debris particles which are generated are difficult to remove from very small IEG. This phenomenon causes the chance of short circuit between electrodes and creates the non-uniform discharge during micro-EDM. With the implementation of ultrasonic vibration, the dielectric can be circulated even in the narrow gap as the assisted ultrasonic vibration produces a pumping effect and enhances the circulation of dielectric at inter electrode gap which reduces the machining time, reduces the amount of electrode wear, improves the material removal rate and reduces the chances of micro-cracks generation on machined surface [37–39]. The ultrasonic vibration assisted micro-EDM helps to produce high aspect ratio micro-holes efficiently compared to normal micro-EDM without ultrasonic vibration. Moreover, the material removal rate increases significantly with less electrode wear ratio and quality of machined surface and dimensional accuracy has been improved [39]. The ultrasonic vibration of work material in micro-EDM shows a drastic improvement. The machining efficiency has been increased up to 8 times when compared to traditional micro-EDM process during machining of stainless steel of thickness 0.5 mm and up to 60 times during the machining of Nitinol [40, 41]. Figure 3.15 shows the ultrasonic vibration assisted micro-EDM process along with different tool tip positions and IEG at different positions of vibration. The powder mixed dielectric always contributes on the performance of micro-EDM process. During vibration assisted powder mixed

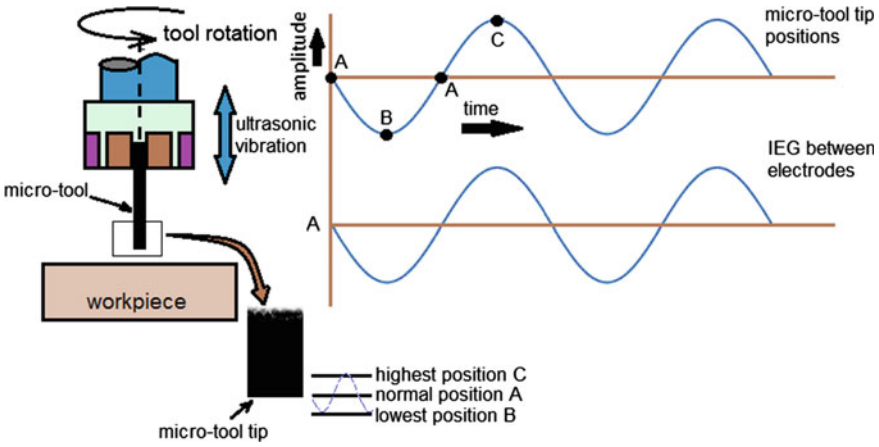

Fig. 3.15 Schematic of ultrasonic vibration assisted micro-EDM process with amplitude of vibration

micro-EDM, the adhesion of powder or abrasives in the narrow gap between the micro tool and the work material occurs. Therefore, implementing ultrasonic vibration during powder mixed micro-EDM, MRR increases significantly as it enhances the dielectric circulation in the machining zone [42]. The drawbacks due to arcing and short circuits in micro-EDM can be reduced substantially when assisted with ultrasonic vibration as the number of normal pulses and the average pulse energy increases [43, 44]. The machining time of micro-EDM can be reduced significantly with increase in vibration frequency at constant amplitude which significantly reduces the start-up process. The vibration between the micro-tool and the work material obstructs the arc which ends the arcing state [45]. Thus, the total duration of arcing event reduces and decreases with increase in vibration frequency. Figure 3.16 shows the comparison of quality of blind micro holes produced with and without ultrasonic vibration (frequency of 6 kHz and amplitude of 3 µm) [46]. The comparison shows the improvement in the dimensional accuracy by 10.5 µm. Furthermore, the micro-hole produced without vibration is larger (diameter is 201.5 µm) than micro-hole generated with ultrasonic vibration (diameter is 191 µm) and this result indicates that the electrode wear is less in ultrasonic assisted micro-EDM process. The recast layer formation has been always a drawback during micro-EDM process. Due to better dielectric circulation in the machining zone, the debris removal from narrow gap due to ultrasonic vibration is improved and results in less re-solidification or recast layer [37]. Moreover, this leads to thinner heat-affected zone produced around the machined cavities. The ultrasonic vibration assisted micro-EDM machining not only shows the improvement in the process performance when used with conventional and powder mixed dielectric, but it also shows the tremendous contribution during dry EDM/micro-EDM. The improvement in MRR has been reported when compared to gas based EDM and liquid

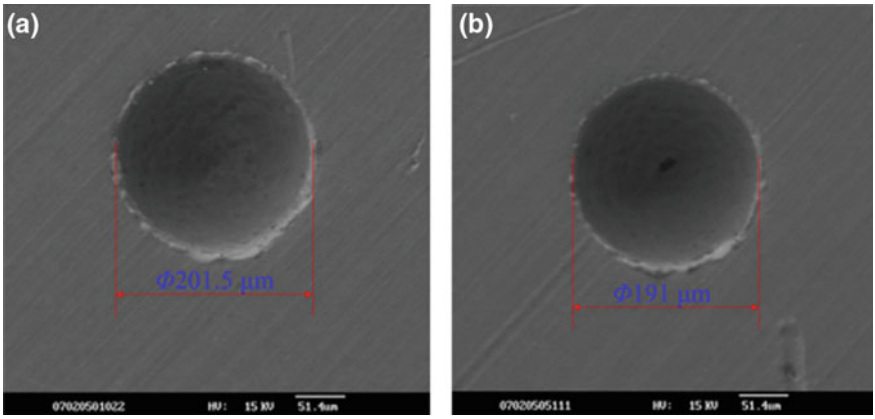

Fig. 3.16 SEM images of blind holes generated **a** without ultrasonic vibration and **b** with vibration [46]

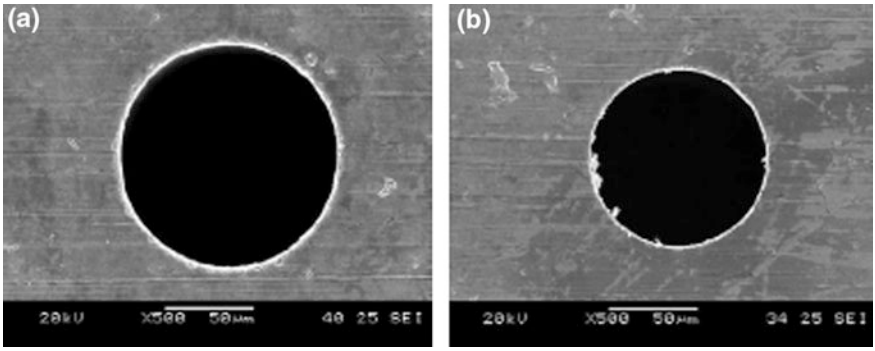

Fig. 3.17 SEM images of micro-hole of **a** entrance and **b** exit side machined with ultrasonic vibration micro-EDM [48]

based EDM without vibration [47]. The reduction in taperness has been achieved when micro-hole is machined with the aid of ultrasonic vibration. Figure 3.17 shows SEM images of micro-hole of entrance (diameter of 122 μm) and exit (diameter of 106 μm) side when machined with ultrasonic assisted micro-EDM [48]. The difference in the diameter (16 μm) is due to secondary discharge and wear of micro-tool.

3.10.2 Utilization of Non-hydrocarbon Dielectrics

In most of the conventional EDM systems, hydrocarbon oil kerosene is used. However, during machining with kerosene dielectric, it creates several drawbacks

such as degradation of dielectric properties, pollution of air, and adhesion of carbon particles on the work surface etc. Due to these, unstable machining operation takes place and results in inefficient performance during micro-EDM. Thus, it is the task of manufacturer engineers and research scientists to find out alternate dielectric which can overcome the above-mentioned drawbacks. De-ionized water is one of the non-hydrocarbon dielectric which can efficiently be used during micro-EDM process. The use of de-ionized water as dielectric does not produce any toxic vapours such as CO and CH_4 as liberated in case of kerosene oil [49]. Compared to kerosene, de-ionized water keeps the machining environment clean and safe. Moreover, de-ionized water supplies oxygen in the machining zone and this promotes stable discharges in IEG. Furthermore, the high degree of fluidity and high cooling rate properties of de-ionized water encourages the debris particles to flush out quickly from IEG and cool the discharge zone quickly and prepares for next discharges.

From the exhaustive review of micro-EDM of Ti–6Al–4V, it is found that very few research investigation were performed on implementing de-ionized water dielectric during micro-hole machining. Further, comparative study on the performance of pure kerosene and pure de-ionized water has not been performed during machining of Ti–6Al–4V alloy. Keeping in view of the requirements and developmental research issue for improving the micro-EDM performance measures, a well-planned research methodology has been designed to investigate the influence of various dielectrics such as kerosene and de-ionized water on various micro-EDM performances such as material removal rate, tool wear rate, overcut, diameteral variance at entry and exit hole (DVEE) and machined surface topography through various test results and scanning electron microscope (SEM) micrographs.

(a) **Experimental details and machining conditions**

The experiments are performed on a traditional die sinking EDM (model: series 2000, EMS-5535-R50, ZNC EDM machine, Manufacturer: Electronica Machine Tools Pvt. Ltd., Pune, India). This EDM set up consists of (i) Spark generator unit, (ii) Z axis unit with servo feed mechanism, (iii) X-Y table unit and (iv) Dielectric pumping and filtering unit. Figure 3.18a, b shows the photographic view of the main components of micro-EDM set up used in this experimental study. When machining experiments were carried out using de-ionized water, a separate dielectric chamber with separate pump, and pressure-regulating valve and filter were used to circulate the dielectrics without affecting dielectric supply system of the main machine. Figure 3.18c shows the developed external dielectric supply system to circulate dielectrics during micro-EDM experiments. Through micro-holes were machined on Ti–6Al–4V plates of size 13 × 15 × 1 mm. Cylindrical shaped tungsten electrodes with flat front of diameter 300 μm were used as tool. Tables 3.1 and 3.2 show the chemical compositions and physical as well as mechanical properties of titanium alloy (Ti–6Al–4V), respectively. Electrical resistivity of boron carbide is in the range of 0.1–10 Ω-cm. As the micro-EDM performances are affected mostly by peak current (Ip) and

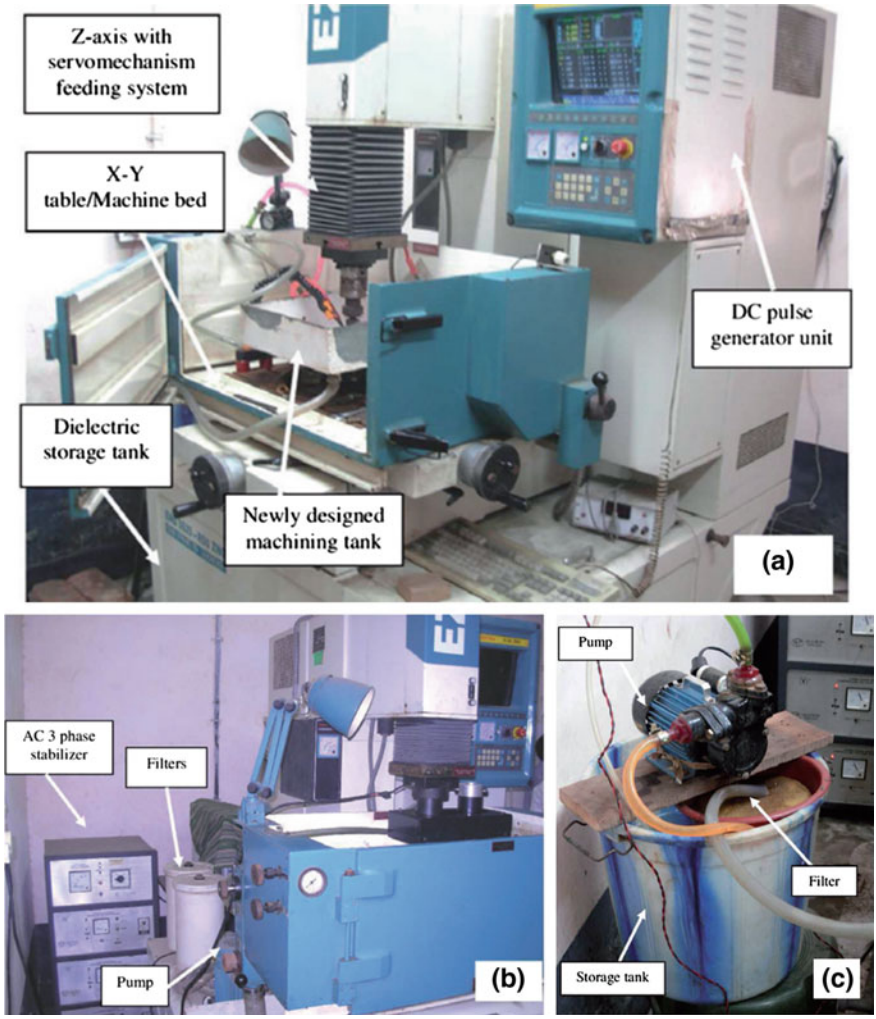

Fig. 3.18 Photographic views of **a** and **b** EMS-5535-R50, ZNC EDM machine **c** external dielectric supply system for circulating de-ionized water

pulse-on-time (Ton) during machining of Ti–6Al–4V alloy [24, 50], so influence of these two predominant process parameters were considered as the varying parameters keeping other process parameters like flushing pressure (Pr), duty factor (t) as constant during machining with each dielectrics.

In this research investigation, experimentations have been carried out at various peak current settings i.e. 0.5, 1, 1.5, 2 A employing kerosene and deionized water. The details of the machining conditions and other parameter details are enlisted in Table 3.3. In this research study, micro-EDM characteristics such as material removal rate (MRR), tool wear rate (TWR), overcut (OC) and diameteral variance

Table 3.1 Compositions of Ti–6Al–4V superalloy

Element	Percentage
Aluminium	5.5–6.75
Carbon	≤ 0.10
Iron	≤ 0.50
Hydrogen	≤ 0.015
Nitrogen	≤ 0.05
Oxygen	≤ 0.45
Other	<0.4
Vanadium	3.5–4.5
Titanium	Balance

Table 3.2 Physical and mechanical properties of Ti–6Al–4V

Property	Typical value
Density (g/cm^3)	4.42
Melting range (°C±15 °C)	1649
Specific heat (J/kg °C)	560
Thermal conductivity (W/m-K)	7.2
Tensile strength (Mpa)	897
Elastic modulus (GPa)	114
Hardness Rockwell C	36

in entry and exit (DVEE) were considered as the machining characteristics. Material removal rate was calculated using Eq. (3.2). Similarly, tool wear rate is calculated using Eq. (3.3). A high precision weighing machine (Manufacturer: Mettler Toledo, Switzerland, Least measurable weight = 0.01 mg) is used to measure various weights of workpiece and micro-tools. The overcut of micro-hole machined is measured using Eq. (3.4). A high precision measuring microscope (Manufacturer: OLYMPUS, Japan, Model: STM6, minimum measurable dimension = 0.5 μm) is used to measure all the dimensions of micro-hole diameters as well as of micro-tool. Experimentation were conducted at various micro-EDM parametric combinations, measured and calculated the performance criteria. The discussion and analysis of various test results are described in the following sections.

(b) **Results and discussion**

In this section, a detailed comparison of various machining performance characteristics has been performed for the investigation of influence of dielectric liquid with kerosene and de-ionized water in micro-EDM for micro machining of titanium alloy (Ti–6Al–4V). Figure 3.19 depict the comparison of the material removal rate (MRR) using two different dielectrics such as kerosene and de-ionized water varying peak current (Ip) and pulse-on-time (Ton). The material removal rate (MRR) is much more using de-ionized water than the kerosene throughout the considered range of pulse duration and increase of peak current. When machining is done with kerosene, as the dielectric fluid is kerosene which is a chemical compound of carbon and hydrogen, decomposes and produces a layer of titanium

Table 3.3 Experimental condition for through micro-hole machining on Ti–6Al–4V alloy

Condition	Description
Workpiece material (anode)	Ti–6Al–4V plate of size 13 mm × 15 mm and thickness of 1 mm
Tool electrode (cathode)	Solid tungsten micro-tool, diameter of 300 μm
Dielectric fluids	Kerosene, de-ionized water
Peak current (A)	0.5, 1, 1.5, 2
Pulse-on-time (μs)	1, 2, 5, 10, 20
Duty factor (%)	95
Flushing pressure (kgf/cm^2)	0.5
Resistivity of pure de-ionized water (megohm-cm)	4.2

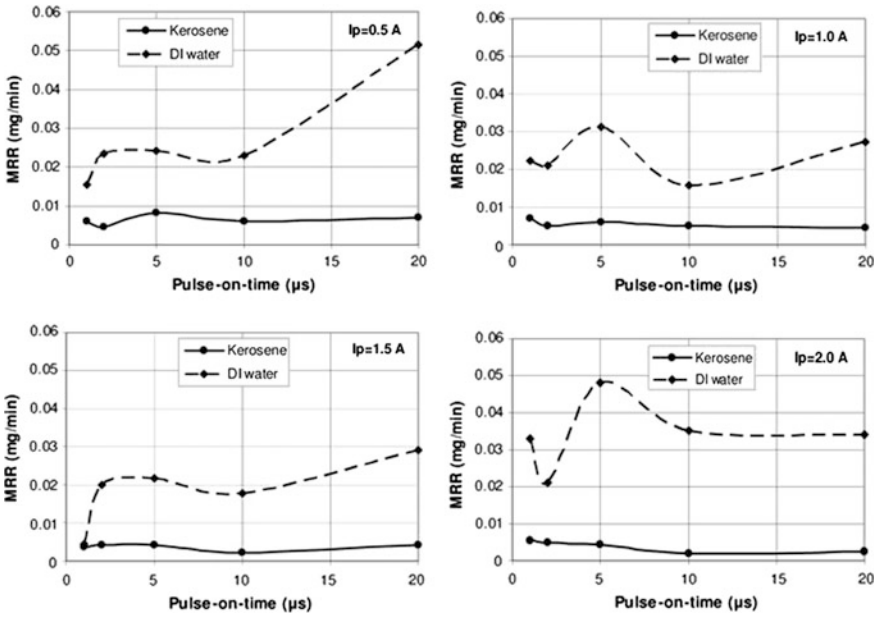

Fig. 3.19 Influence of different dielectrics on the material removal rate (MRR) with varying pulse-on-time (Ton)

carbide (TiC) on the workpiece surface. But, when using de-ionized water, the water decomposes and a layer of titanium oxide (TiO_2) is produced on the machined surface. Since, TiC has a higher melting temperature (3150 °C) than that of TiO_2 (1750 °C), a large discharge energy is required for improving the material removal rate using kerosene. Also, the size of debris formed during machining with kerosene is less compared to machining with de-ionized water, thus improving the material removal rate.

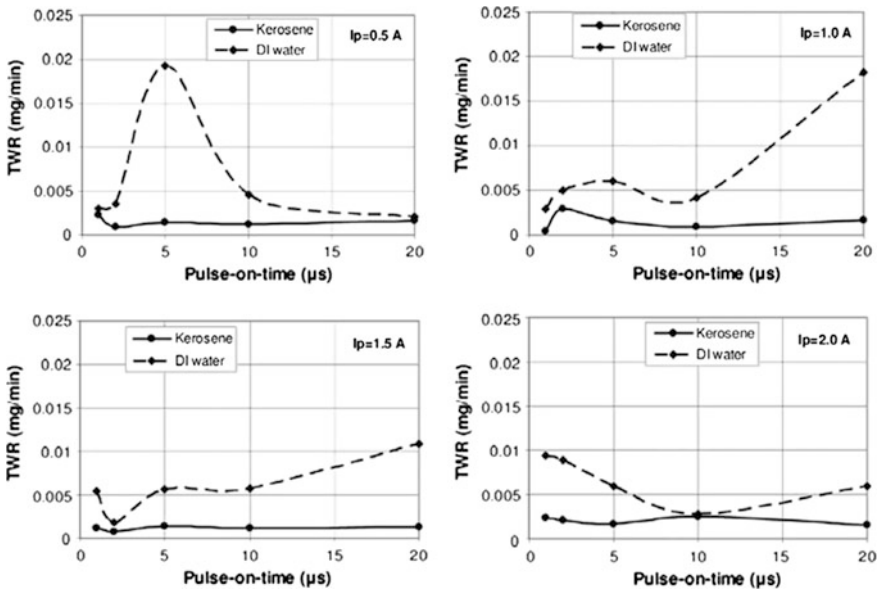

Fig. 3.20 Influence of different dielectrics on the tool wear rate (TWR) with varying pulse-on-time (Ton)

Figure 3.20 shows the comparison of the tool wear rate (TWR) using two different dielectrics such as kerosene and de-ionized water varying peak current (Ip) and pulse-on-time (Ton). It is seen from the figure that the tool wear rate (TWR) is high using de-ionized water compared to machining with kerosene. When using kerosene as the dielectric, it decomposes in the high discharge energy and produces carbon particles that stuck or adhere to the surface of the electrode. These carbon particles restrict the rapid wear of the tool. So, the tool wear rate (TWR) is less while using kerosene as dielectric. On the other hand, when using deionized water, no carbon adhere to the tool electrode surface, thus TWR is higher enough with de-ionized water.

Figure 3.21 shows the comparative study of the overcut (OC) using two different dielectrics i.e. kerosene and de-ionized water with varying peak current (Ip) and pulse-on-time (Ton). From the figures, it is clear that the overcut of the machined micro-holes is larger when using de-ionized water for the pulse duration of 1 and 2 µs when machining is done by varying peak current. But at higher pulse duration the overcut of the micro-holes is larger when using kerosene as the dielectric. When deionized water is used, it releases oxygen decomposed from water. This oxygen influences the machining stability and helps to form more debris. These debris particles ejected through the short gap of tool surface and micro-hole walls. Thus increasing secondary sparking, resulting in higher overcut compared to kerosene. But at higher pulse duration, the machining stability and efficiency increases due to more pulses per cycle, resulting higher overcut with kerosene compared to

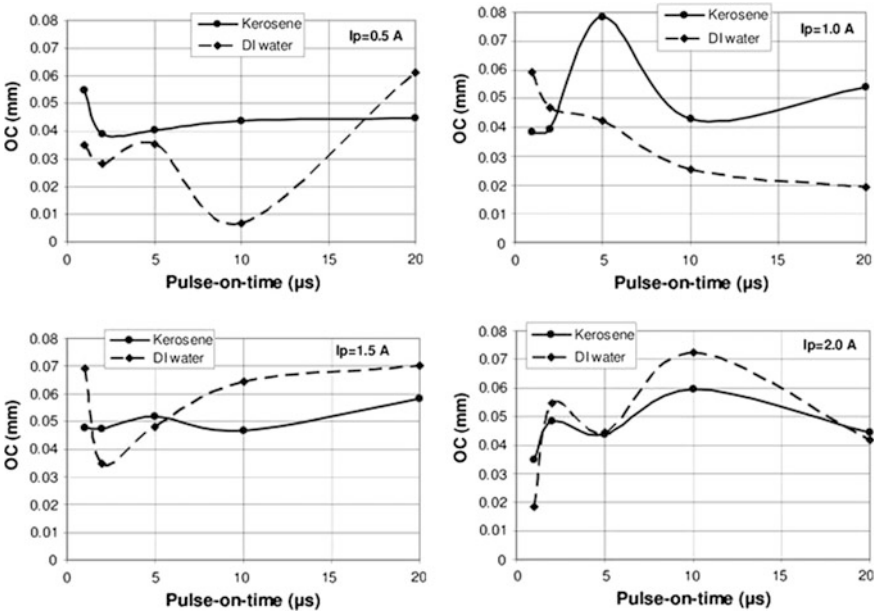

Fig. 3.21 Influence of different dielectrics on the overcut (OC) with varying pulse-on-time (Ton)

de-ionized water. When the overcut is analyzed with the increase of peak current it is found that a high peak current results higher overcut with de-ionized water compared to kerosene.

Figure 3.22 shows the comparison of the diameteral variance in entry and exit (DVEE) using two different dielectrics i.e. kerosene and de-ionized water with varying peak current (Ip) and pulse-on-time (Ton), respectively. It can be observed from the figures that DVEE of the micro-holes increases at low discharge duration when varying peak current was employed using de-ionized water as dielectric fluid. But further increase of pulse duration results the decrease of DVEE of the holes with de-ionized water. A straight through micro-hole can be generated at pulse duration of 5 μs and peak current of 1.5 A. On the other hand, DVEE is lower at peak current 0.5 and 1 A employing deionized water compared to kerosene. But, as the peak current increases, the diameter variance increases with de-ionized water. Thus, a straight through micro-hole is not achieved.

After machining of micro-holes utilizing various type of dielectric fluids, the workpiece were carefully polished, cleaned, and etched with a solution of 2.5 ml of HF acid (40%), 5 ml concentration of HNO_3 and 42.5 ml of de-ionized water for examining the surface topography of micro-holes as well as the recast layer formed on the machined micro-hole surfaces with the aid of optical and SEM micrographs. Figure 3.23 shows some optical micrographs of machined micro-holes that were taken using a 10X zoom lens in a precision optical microscope for both pure dielectrics i.e. kerosene and de-ionized water at the machining condition of 1 A

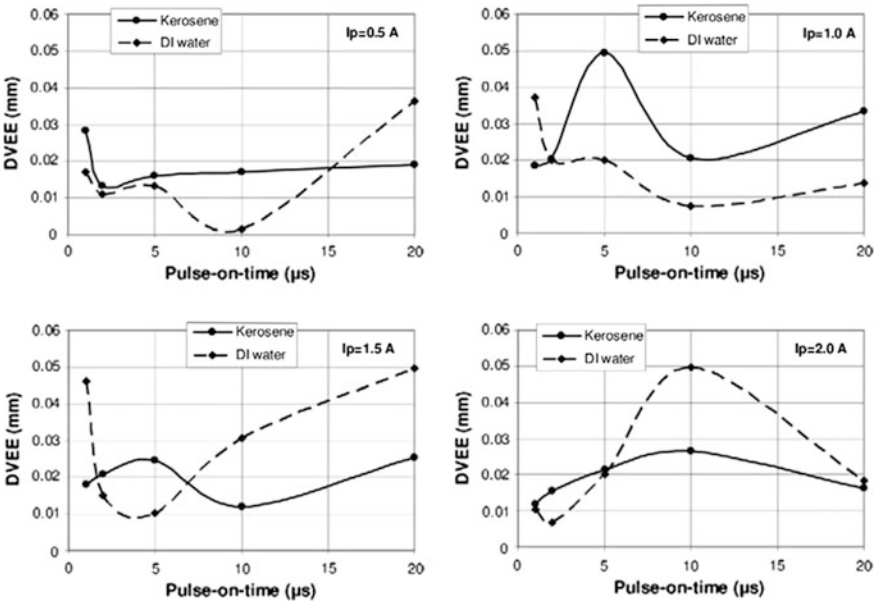

Fig. 3.22 Influence of different dielectrics on the diameter variance between entry and exit (DVEE) with varying pulse-on-time (Ton)

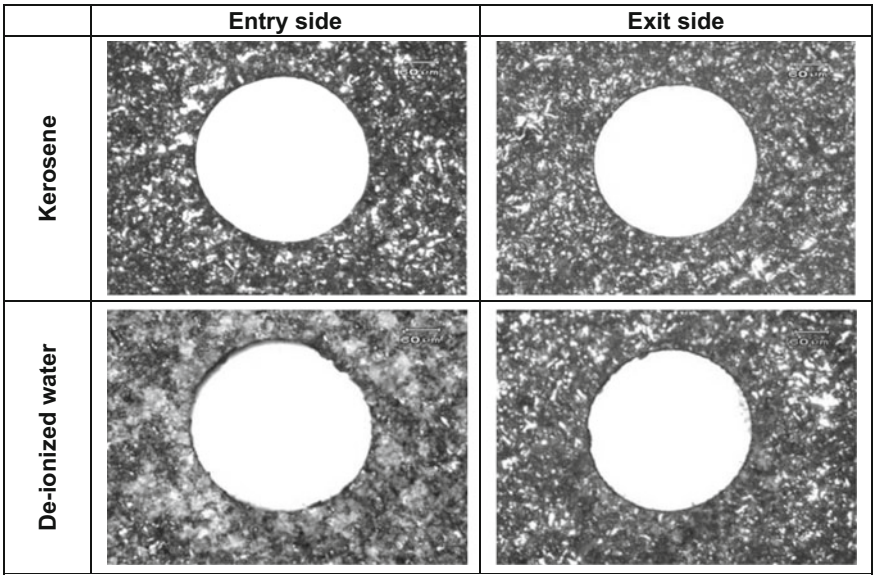

Fig. 3.23 Optical photographs of machined micro-holes with different dielectrics at 1 A/2 µs [51]

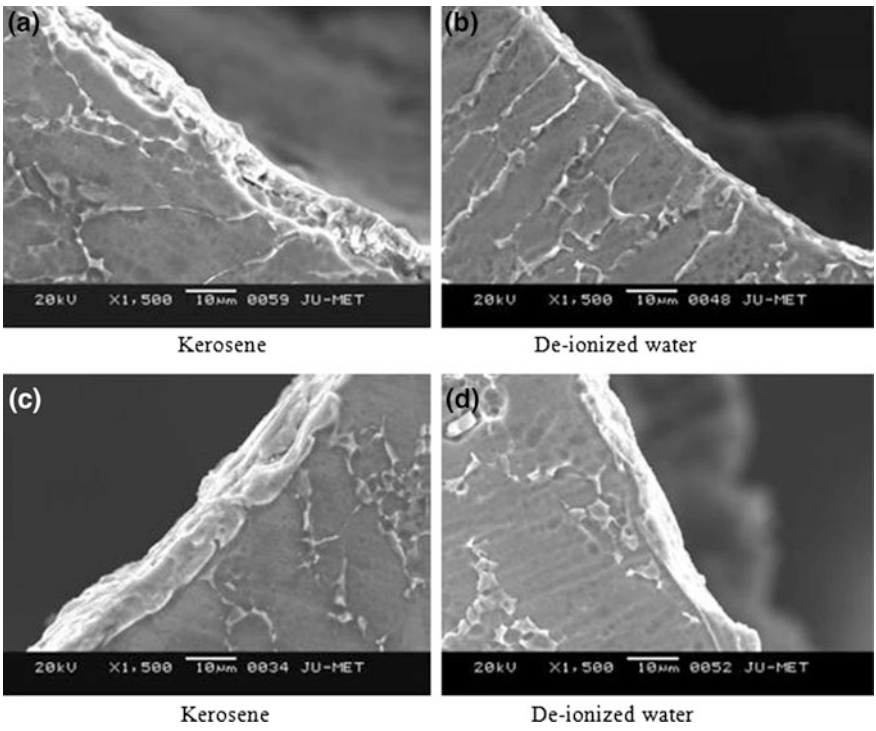

Fig. 3.24 SEM micrographs of white layer formed on micro-hole edge **a** and **b** machined at 0.5 A/1 μs and **c**, **d** machined at 1.5 A/10 μs [51]

peak current and 2 μs pulse duration. It is clear from these figures that kerosene dielectric result in improved quality micro-hole than de-ionized water. In Fig. 3.24, SEM micrographs of the micro-hole's edges are shown to examine the white/recast layer formation using kerosene and de-ionized water. The thickness of the white layer is much lower using de-ionized water compared to kerosene. Moreover, with increase of the pulse-on-time, the thickness of the white layer increases. As pulse duration increases, the effective machining time also increases. Therefore, more debris is generated and this debris adheres to the micro-hole surface and resolidified as deionized water has high cooling rate than kerosene.

3.10.3 Abrasive Mixed Dielectric in Micro-EDM

In micro-EDM, debris in the inter electrode gap facilitates the ignition process and further increases the gap size and overall flushing conditions [52]. Absence of debris particles in the gap can results arcing between the electrodes and it further results in lack of precise feeding mechanism. However, excess debris leads to uneven discharge and short-circuiting. Some debris particles in the machining gap

provide better discharge transitivity, gap size, breakdown strength, and deionization [53]. From the past research, it is revealed that most of the research has been performed on EDM employing powder mixed dielectrics. However, no research was reported to use powder mixed dielectric during micro-EDM of Ti–6Al–4V. Thus, in the present experimental study, detailed analysis has been carried out to investigate comparatively the influence of mixing boron carbide powder in kerosene and de-ionized water during micro-hole machining in micro-EDM on Ti–6Al–4V material. This B_4C powder has some excellent physical and chemical properties such as high chemical resistance and hardness, excellent wear and abrasion resistant etc. These exceptional characteristics of boron carbide may provide effective and efficient discharge conditions at the machining zone and also enhancement in above-mentioned machining performances. Electrical resistivity of boron carbide is in the range of 0.1–10 Ω cm. As B_4C abrasive lie in a transition zone between good conductors and isolators, the potential difference as well as the plasma channel produced in the micron sized inter electrode gap can make the abrasive to conduct thermoelectric power in the machining zone [54, 55]. Boron carbide is characterized by a relatively wide gap in its forbidden band, a low thermal conductivity, and a high thermoelectric power. These properties make it a potentially useful material for high-temperature thermoelectric energy conversion compared to silicon carbide as well as tungsten carbide abrasives.

(a) **Experimental details and machining conditions**

As micro-EDM process uses discharge energy in the range of 5–150 µJ, so there is a little chance to melt and evaporate the B_4C particles due to discharge in the inter electrode gap. It was observed in the optical measuring microscope that the powder particles comprise of mixture of different shapes and sizes ranging from 8 to 20 µm. When, Boron carbide (B_4C) powder-mixed de-ionized water was applied in the machining zone, most of the particles, which are more than 10 µm in size, get accumulated at the base of machining zone because of self-weight of particles even though a motor driven stirrer was applied to provide turbulence in powder mixed dielectrics in the machining tank. Hence, the effective average particle size that may involve in the machining phenomena at the micro-machining zone ranges from 8 to 10 µm during micro-EDM. Therefore, the average size of B_4C particles which actively take part in machining is in the range of 8–10 µm. The thermo-physical properties of boron carbide powder are enlisted in Table 3.4. B_4C powder additive

Table 3.4 Thermo-physical properties of Boron carbide (B_4C) additives

Property	Typical value
Density (g/cm^3)	2.52
Melting point (°C)	2445
Electrical conductivity (at 25 °C) (S)	140
Thermal conductivity (at 25 °C) (W/m K)	30–42
Young's modulus (GPa)	450–470
Hardness (Knoop 100 g) (kg mm^{-2})	2900–3580
Specific heat (J K^{-1} kg^{-1}) (at 25 °C)	950

of size 8–10 μm and of concentration 4 g/l was added to pure kerosene and deionized water when experimentations were performed with powder-mixed dielectrics. This particular concentration of additive in dielectrics has been selected based on past research studies on powder mixed dielectrics in EDM [56, 57]. The same micro-EDM machine was utilized for this experimental investigation. When experiments are done with powder mixed kerosene and powder mixed de-ionized water, a separate dielectric chamber with separate pump, and pressure-regulating valve and filter were used to circulate the dielectrics without affecting dielectric supply system of the main machine. When machining was done with powder-mixed dielectric, the external filter unit was removed, and a magnetic field was employed to remove the machining debris from the dielectrics. In this research study, micro-EDM characteristics such as material removal rate (MRR), tool wear rate (TWR), overcut (OC), diameteral variance in entry and exit (DVEE) were considered as the machining characteristics. The discussion and analysis of various test results are described in the following sections.

(b) **Results and discussion**

Figure 3.25 shows the comparative plots of the material removal rate (MRR) using different dielectrics such as pure kerosene, pure de-ionized water and Boron Carbide (B_4C) mixed dielectrics powder for varying pulse-on-time (Ton) at different peak currents (Ip). This figure reveals that MRR is high with de-ionized water

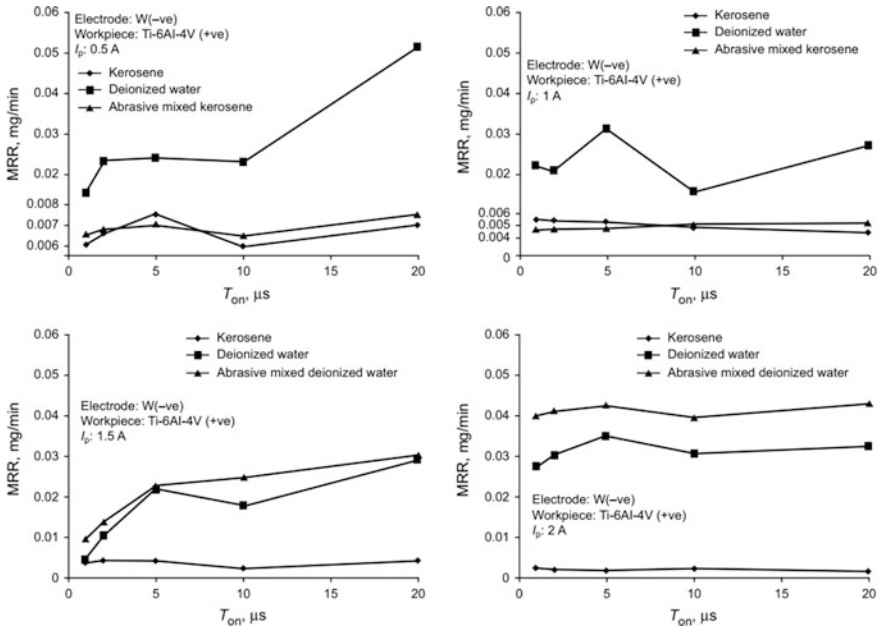

Fig. 3.25 Variation of material removal rate (MRR) with pulse duration (Ton) at various fixed peak current (Ip) for different dielectrics [51]

than kerosene for all considered settings of pulse duration and peak current during experimentation. Additionally, when machining is done by mixing B_4C powder additives in kerosene dielectric it is clearly seen that MRR increases with the increase of pulse duration at constant peak current of 1.5 and 2 A. Also the MRR with powder mixed dielectrics is larger compared to machining with pure kerosene and de-ionized water at higher pulse duration discharge settings. The increase of MRR with the increase of pulse duration using B_4C mixed kerosene is due to increase of spark discharge time i.e. longer effective machining time per pulse. The presence of boron carbide additive in kerosene further helps in uniform distribution of discharge energy and better conduction of discharge current thereby enabling better machining condition. When B_4C powder was applied to de-ionized water, it is seen that MRR is more using additive compared to pure deionized water at peak current 1.5 and 2 A. The same reason is applicable here also for the increase of MRR as of additive mixed kerosene. So, it is concluded that the addition of carbide powder particles in dielectrics prevails better machining efficiency than the pure dielectrics due to uniform distribution of discharge energy in the machining zone.

In Fig. 3.26 comparative results of tool wear rate (TWR) with pulse duration at different pulse discharge with various constant peak current are shown employing kerosene, de-ionized water and B_4C powder mixed dielectrics. This figure reveals that TWR is high using de-ionized water compared to machining with kerosene dielectric. Furthermore, it is revealed from the same figure that tool wear rate

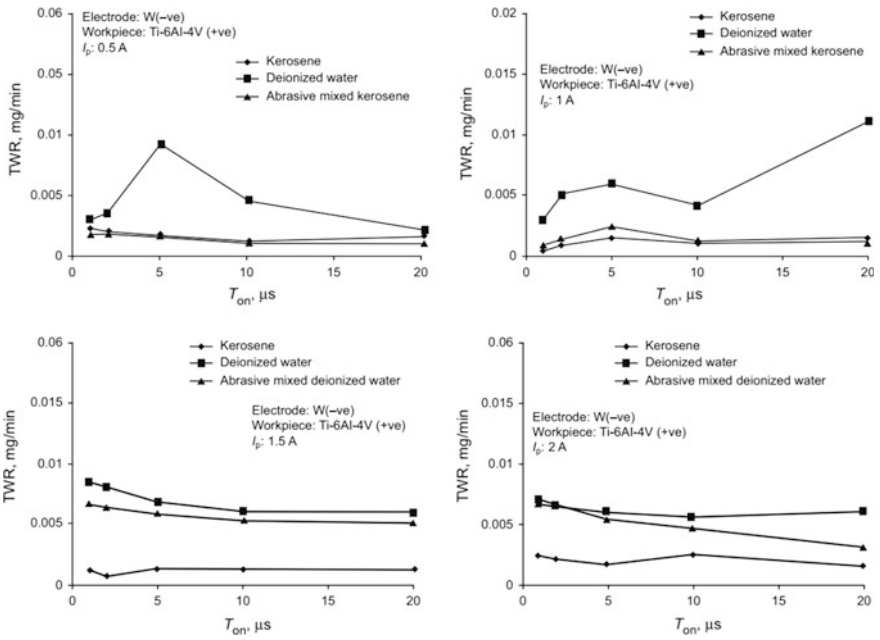

Fig. 3.26 Variation of tool wear rate (TWR) with pulse duration (Ton) at various fixed peak current (Ip) for different dielectrics [51]

associated with B_4C mixed kerosene is less compared to machining with pure kerosene at peak current of 0.5 and 1 A. When machining is done with boron carbide abrasive mixed kerosene dielectric, the tool wear is less due to the presence of more number of carbon particles evolving from the decomposition of kerosene dielectric as well as boron carbide abrasive in the machining zone. From the same figure it is observed that at fixed 1 A peak current tool wear rate is lesser than at fixed 0.5 A current setting using additive mixed kerosene. This is due to the fact that the higher discharge energy results in more decomposition of kerosene and it further generates more carbon which in turn adheres onto the tool surface preventing secondary sparking. Although higher peak current i.e. 2 A produces more discharge energy, but that results in more current density and subjects the tool electrode under large thermal stresses. The powder mixed de-ionized water results in less tool wear rate at 2 A compared to 1.5 A due to more deposition of carbon particles from B_4C additives. It is also found that machining combined with boron carbide powder mixed deionized water results in less tool wear compared to pure de-ionized water due to adhesion of carbon particles from boron carbide powder on the tool surface, which restrict tool wear to certain extent.

The comparative plots of overcut (OC) of micro-holes on Ti–6Al–4V employing kerosene, deionized water and B4C abrasive mixed with these dielectrics are shown in Fig. 3.27 when pulse duration was varied for fixed different peak current. It is observed from these figures that the overcut of the machined micro-holes is less

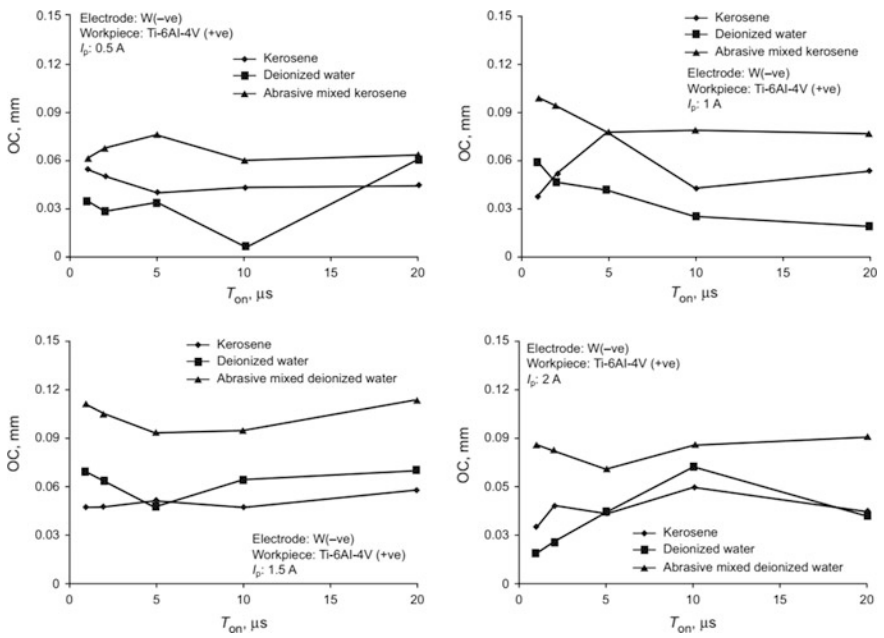

Fig. 3.27 Variation of overcut (OC) with pulse duration (Ton) at various fixed peak current (Ip) for different dielectrics [51]

when dielectric was de-ionized water for peak current setting of 0.5 and 1 A. However, at higher peak current i.e. 1.5 and 2 A, overcut is more in case of de-ionized water compared to pure kerosene dielectric. In addition, when B_4C additive was used in dielectrics, it is found that OC is larger with both powder mixed dielectrics compared to pure dielectrics. It is so because the suspended additive particles remove the molten layer from the machining zone and further reduce the formation of thick white layer, resulting larger OC. It is also revealed that OC decreases with increase in pulse duration while using B_4C suspended kerosene as dielectric. It is due to decrease of overall machining time i.e. faster machining. However, larger OC is found in case of B_4C mixed deionized water as dielectric because of secondary sparking.

Figure 3.28 shows the comparative outcomes of diameteral variance at entry and exit (DVEE) using kerosene, de-ionized water and boron carbide powder mixed with these dielectrics. It is found from this figure that DVEE of the micro-holes is lower employing de-ionized water compared to kerosene as dielectric fluid at lower peak current i.e. 0.5 and 1 A. However, at higher peak current i.e. 1.5 and 2 A, DVEE is larger using de-ionized water. It is also found that boron carbide powder mixed kerosene results in large DVEE compared to pure kerosene at low peak current of 0.5 and 1 A. As the machining progresses, the additive boron carbide particles creates more carbon adhesion on the work surface, that further results in

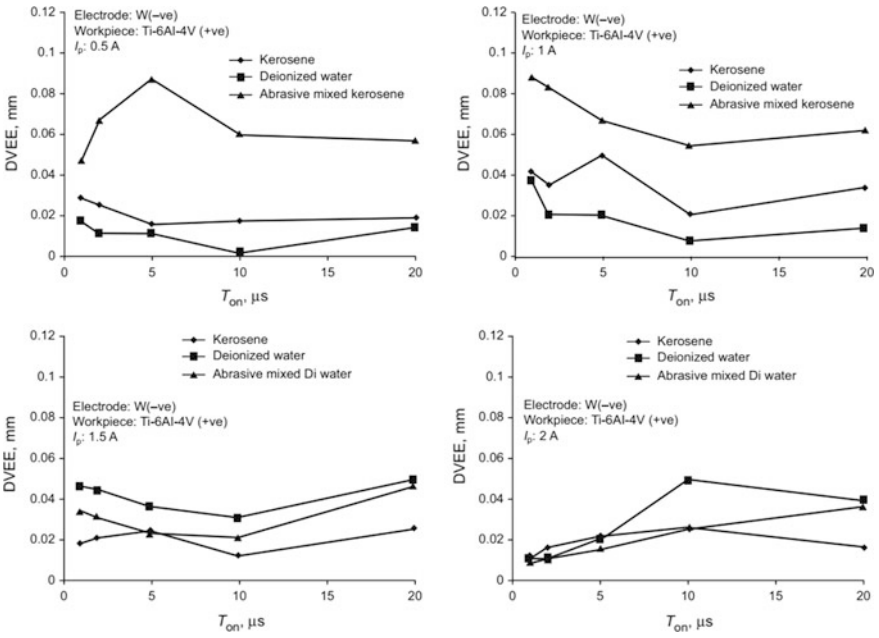

Fig. 3.28 Variation of diameteral variance at entry and exit (DVEE) with pulse duration (Ton) at various fixed peak current (Ip) for different dielectrics [51]

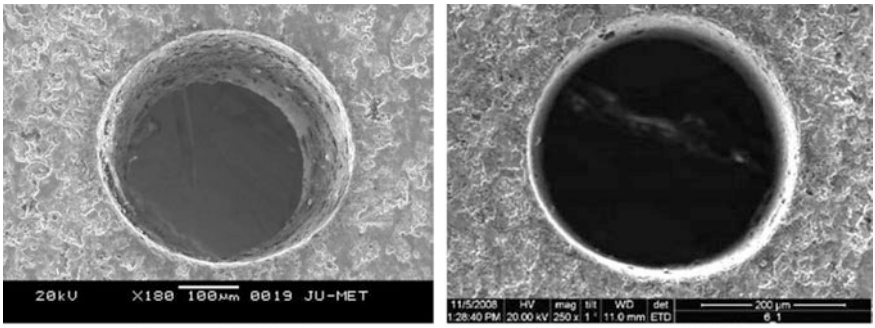

Fig. 3.29 SEM micrographs of machined micro-holes using powder mixed dielectrics [51]

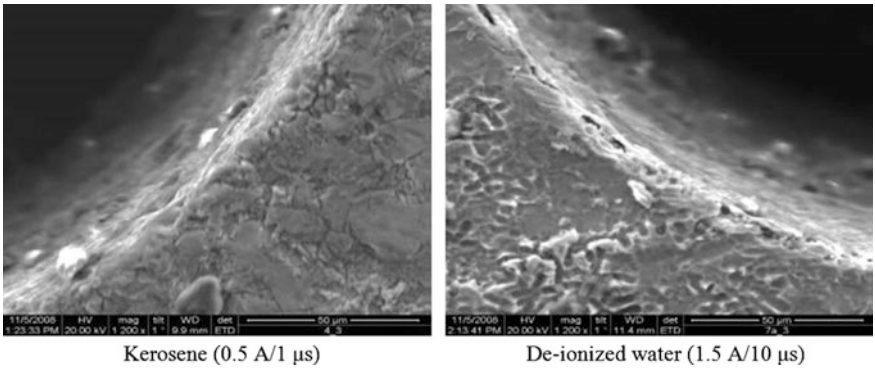

Fig. 3.30 SEM micrographs of white layer of machined micro-hole's edges using powder mixed dielectrics [51]

lower material removal at exit side of micro-hole and greater variance in entry and exit diameters. But, when B_4C additive mixed de-ionized water is used at higher peak current of 1.5 and 2 A, the powder particles help in uniform distribution of discharge energy which in turn leads to better dimensional accuracy micro-holes compared to pure de-ionized water.

Figure 3.29 shows SEM micrographs of the inner surface of machined micro-hole using powder mixed kerosene and de-ionized water at parametric combinations of 1 A/5 µs and 2 A/10 µs of peak current and pulse-on-time. It is revealed from these micrographs that with more discharge energy, inaccurate micro-hole is generated using powder mixed de-ionized water due to more secondary sparking phenomena. However, smooth inner surface is produced using powder mixed de-ionized water than powder mixed kerosene. In Fig. 3.30, SEM micrographs of micro-hole's edge are viewed for examining the recast/white layer formation during micro-hole machining. It is revealed from these figures that the

recast layer formed on the edges is very less than using pure dielectrics. It is due to the fact that the additive particles help to remove the molten debris and restrict to form thick white layer on machined micro-hole edges.

3.10.4 Rotation of Micro-tool Electrode

During micro-EDM process, the machining performances can be enhanced by implementing micro-tool electrode rotation about its axis. While rotating the micro-tool, flushing out of debris particles from very narrow IEG occurs quickly due to generation of tangential force in the machining zone. This leads to effective and efficient discharge between the electrodes. In this section, the effects of peak current (Ip), pulse-on-time (Ton) and rotational speed of the micro-tool electrode are explored during micro-hole machining in micro-EDM process.

(a) **Experimental method and machining conditions**

The experiments were conducted using the same ZNC R50 EDM machine to investigate the effects of rotation of electrode in respect of material removal rate (MRR), tool wear rate (TWR), overcut (OC) and DVEE on Ti–6Al–4V workpiece of 1 mm thickness with a brass electrode of 300 μm in diameter. During machining, kerosene is used as dielectric fluid. For rotating the tool electrode, tool rotational attachment has been used in which the rotational speed can be varied between 1 and 300 rpm in a resolution of 2 rpm. The range of peak current (Ip) and pulse-on-time (Ton) selected were 0.5–2 A and 1–20 μs respectively. The experiments were conducted in two stages: (i) varying only peak current from 0.5 to 2 A keeping pulse-on-time, duty factor and flushing pressure as constant at 10 μs, 95%, 0.5 kgf cm^{-2} respectively and (ii) varying only pulse-on-time from 1 to 20 μs keeping peak current, duty factor, flushing pressure constant at 1 A, 95% and 0.5 kgf cm^{-2} respectively with stationary and rotating electrode with a rotational speed of 150 rpm in each case. The peak current has been fixed at 1 A because for micro-machining, very low current density is not sufficient to melt and vaporize the work material and very high current density leads to higher TWR and larger thermal damage of the workpiece surface. On the other hand, pulse-on-time is fixed at 10 μs because short duration is more beneficial for micromachining as it helps in reducing the tool wear. A moderate rotational speed of the electrode has been selected i.e. 150 rpm after conducting trail runs of experiment, because this helps in easy removal of debris from the machining zone and keeps the tool wear at minimum.

(b) **Results and discussion**

Utilizing the micro-tool electrode rotating facility with developed tool holder, the experiments were conducted to study the effects of micro-EDM parameters on process criteria namely material removal rate (MRR), tool wear rate (TWR), overcut (OC) and diameteral variation at entry and exit (DVEE) of the machined micro-holes. The variations of MRR with peak current (Ip) and pulse-on-time

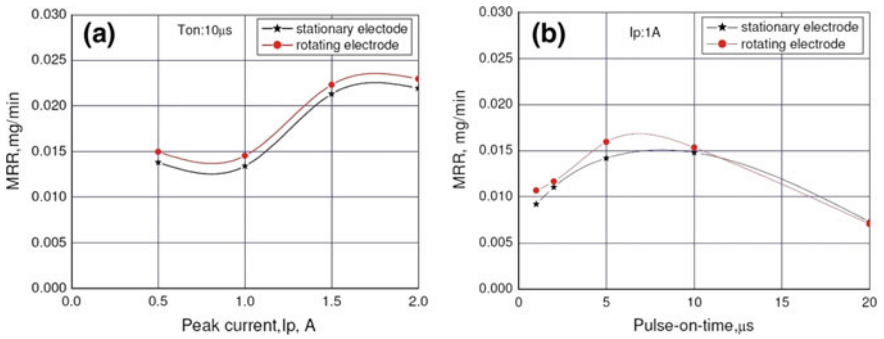

Fig. 3.31 Variation of MRR with **a** peak current and **b** pulse-on-time [58]

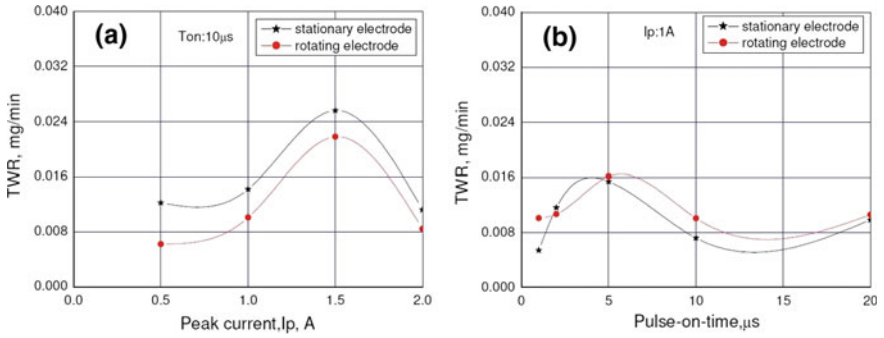

Fig. 3.32 Variation of TWR with **a** peak current and **b** pulse-on-time [58]

(Ton) with stationary and rotating electrode are shown in Fig. 3.31a, b, respectively. It is observed from the graph that MRR increases with increase in peak current as was expected for both stationary and rotating electrodes. Since higher peak current leads to higher discharge energy, so it results in increase of MRR. It is also observed from the same figure that with rotating electrode higher MRR is achieved. The higher MRR with rotating electrode may be attributed to better removal of sludge and carbonized particles from the machining zone due to centrifugal force of rotation. This improved sludge removal due to rotating effect of electrode helps in exposing the actual machining surface, which in turn improves the overall machining condition leading to higher MRR. Thus, for maximum MRR from within the considered range of parametric setting, the best parametric combination in the present case study is 2 A/10 μs/0.5 kgf cm^{-2}/95%/150 rpm.

Figure 3.32a, b respectively show the variations of TWR with peak current (Ip) and pulse-on-time (Ton) with stationary and rotating electrode. It can be observed from the graph that TWR increases as the peak current increases from 0.5 to 1.5 A. However, TWR is observed to decrease from 1.5 to 2 A. The increase in TWR with the increase in peak current can be attributed to the increase in discharge

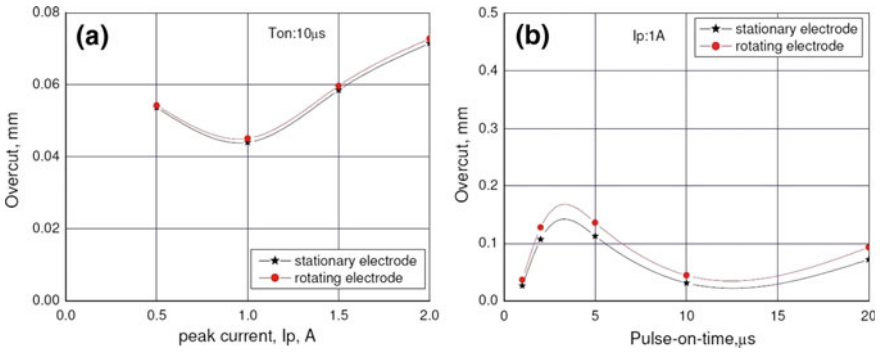

Fig. 3.33 Variation of OC with **a** peak current and **b** pulse-on-time

energy and the rotational effect of the electrode. Further increase in peak current, increases machining efficiency and decreases the tool wear because the tool electrode is subjected to high-energy electric field for shorter duration. Thus, this figure clearly indicates that for micro-hole machining with low TWR, smaller peak current is suitable. Owing to rotational effect, the magnitude of TWR further decreases which is evident from the figure under consideration. This may be attributed to better removal of debris due to the tangential force of rotation. Thus, for least TWR, the best parametric combination within the considered range of parametric settings is 1 A/10 μs/0.5 kgf cm^{-2}/95%/150 rpm.

Figure 3.33a, b respectively show the variations of OC with peak current (Ip) and pulse-on-time (Ton) with stationary and rotating electrode. It is observed from the figure that overcut decreases with the increase in peak current in the range 0.5–1 A which may be attributed to increase in discharge energy with the increase in peak current and enabling faster machining and thereby reducing effective machining time. The reduction in machining time means less exposure of tool electrode to discharge energy which is responsible for tool wear. However, peak current beyond 1 A, overcut has found to increase monotonically. Increase in peak current above 1 A results in larger discharge energy which causes larger MRR resulting in larger overcut. Thus the most suitable parametric combination for least overcut from within the considered range of parametric settings is 1 A/10 μs/95% duty factor/0.5 kgf cm^{-2}/150 rpm.

The variations of DVEE with peak current (Ip) and pulse-on-time (Ton) with stationary and rotating electrode are shown in Fig. 3.34a, b, respectively. It is observed from the same graph that with the increase in peak current, the DVEE decreases. Furthermore, the magnitude of DVEE with rotating electrode is less than that of stationary electrode throughout the considered range of peak current. As the depth of the micro-hole increases, the sparking point shifts radially inward. When the peak current is increased, the thermal energy density increases at the pointed tip of the micro-tools. This high density discharge energy rapidly melts and vapourizes the sharp micro-tool tips and subsequently making the micro-tool end broader

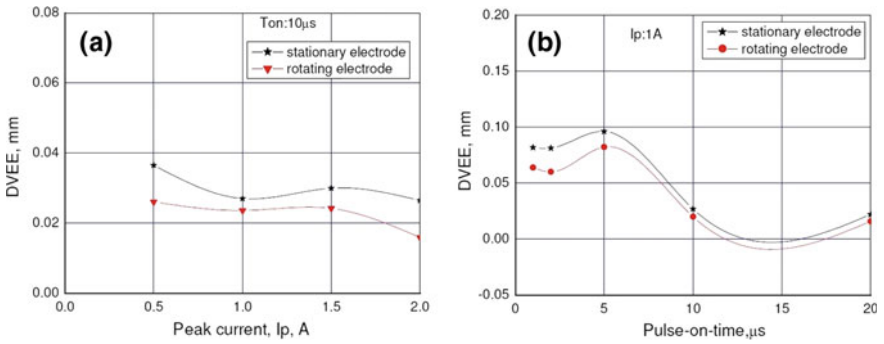

Fig. 3.34 Variation of DVEE with **a** peak current and **b** pulse-on-time

which finally helps in achieving a straight through micro-hole by decreasing DVEE. Further, the rotational speed of the tool helps to remove the sludge and debris efficiently from the machining zone and also reduces the chances of secondary discharge sparking thereby providing stable machining condition for achieving micro-hole with less DVEE. The lowest DVEE achieved is with the parametric combination of 2 A/10 μs/95%/0.5 kgf cm^{-2}/150 rpm.

The improvement in micro-hole geometry with the increase in peak current coupled with rotation of tool electrode may be attributed to better flushing of debris due to rotation of electrode, uniform tool wear, and evenly distribution of discharge energy. Figure 3.35a shows the optical micrographs of micro-hole's diameters at entry and exit machined with parametric setting of 1 A/5 μs/95% duty factor/0.5 kgf/cm^2 i.e. with stationary micro-tool and Fig. 3.35b shows the optical micrographs of micro-hole's diameters at entry and exit machined with parametric setting of 1 A/5 μs/95% duty factor/0.5 kgf/cm^2/150 rpm i.e. with rotating micro-tool. It can be observed from these two micrographs that with rotating tool electrode, straight-through micro-hole can be fabricated.

3.10.5 Reversing Polarity of Electrodes

During micro-EDM process, especially, for micro-drilling operation, the amount of carbon deposition and machining debris increases as micro-hole depth increases and its removal becomes very difficult. Therefore, with the increase in micro-hole depth it becomes necessary to increase the rate of change of polarity in order to facilitate the removal of deposited carbon and debris from the machining zone. In this section, a novel approach has been considered to change polarity of electrodes in reduced time domain. The experimental condition has been designed in a novel way in which the polarity during micro-EDM machining has been changed in a designed fashion in exponential time domain to improve the machining condition, debris removal, machining efficiency to achieve better geometrical accuracy of the

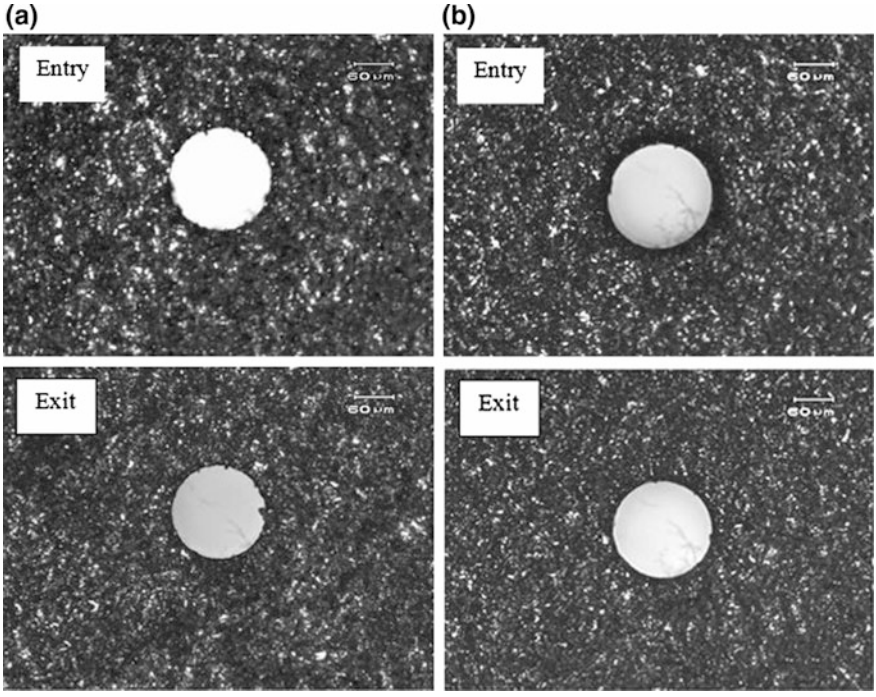

Fig. 3.35 Optical micrographs of micro-holes with **a** stationary and **b** rotating tool electrode machined at 1 A/5 µs/95% duty factor/0.5 kgf/cm^2

micro-hole. In constant polarity machining condition, the job was positive and tool electrode was negative i.e. normal polarity. But, in changing polarity machining condition, the polarity of the job and the tool electrode has been changed in exponential time domain.

(a) **Experimental method and machining conditions**

The machining begins with normal polarity for the first 10 min, then the polarity is changed for next 3 s and again the polarity is switched over to normal polarity and the machining continues for another 9 min before the second change. The time duration of machining with normal polarity reduces after every change and this continues till the through micro-hole is produced on the workpiece. However, the machining with reverse polarity is kept constant at 3 s in each change. The time chart has been prepared after conducting several trail experiments to find out the time required to machine the through micro-hole in 1 mm thick Ti–6Al–4V alloy sheet with 300 µm diameter brass tube electrode. The dielectric fluid used is kerosene. It is learnt from past literatures and experimental investigations in micro-EDM that peak current and pulse-on-time are the most influential parameters. Therefore, these dominating parameters have been selected as process parameters in the present micro-EDM experimentation. To study the effects of pulse-on-time

(Ton) and peak current (Ip), the experimental planning has been carried out firstly by only varying the peak current from 0.5 to 2 A keeping pulse-on-time (Ton), duty factor (t) and flushing pressure (Pr) constant at 10 μs, 95% and 0.5 kgf/cm^2 respectively and secondly by only varying the pulse-on-time (Ton) from 1 to 20 μs keeping peak current (Ip), duty factor (t) and flushing pressure (Pr) constant at 1 A, 95% and 0.5 kgf/cm^2 respectively. The experiments were conducted on the same ZNC R50 EDM machine. Experiment at each parametric setting was conducted three times and the average of the three were considered for calculating material removal rate (MRR), tool wear rate (TWR), overcut (OC) and diameteral variation at entry and exit (DVEE) of the micro-hole.

(b) **Results and discussion**

The variations of MRR with peak current and pulse-on-time with constant and changing polarity, keeping all other process parameters constant i.e. pulse-on-time at 10 μs in case of varying peak current and peak current at 1 A in case of varying pulse-on-time, duty factor at 95%, and flushing pressure at 0.5 kgf/cm^2, shown in Fig. 3.36a, b, respectively. It is noticed from Fig. 3.36a that MRR increases monotonically in both cases with the increase in peak current from 0.5 to 1.5 A but for changing polarity it decreases as peak current increases from 1.5 to 2 A. The magnitude of MRR in both cases is almost equal in the considered peak current range. The low MRR at smaller peak current could be due to lower discharge energy when machining in both constant and changing polarity. However, MRR at changing polarity is low compared with constant polarity as shown Fig. 3.36a due to the change in the position of maximum liberation of heat energy due to sparking. The increase in MRR with increasing peak current is attributed to larger discharge energy. Figure 3.36b shows the variation of MRR with pulse-on-time. It is observed from this figure that the MRR variation is almost opposite in nature for changing and constant polarity at lower pulse-on-time values between 1 and 5 μs. MRR decreases from 1 to 2 μs for constant polarity but in the same pulse-on-time range it increases for changing polarity. In the range from 2 to 5 μs, MRR increases and decreases sharply for constant and changing polarity respectively. However,

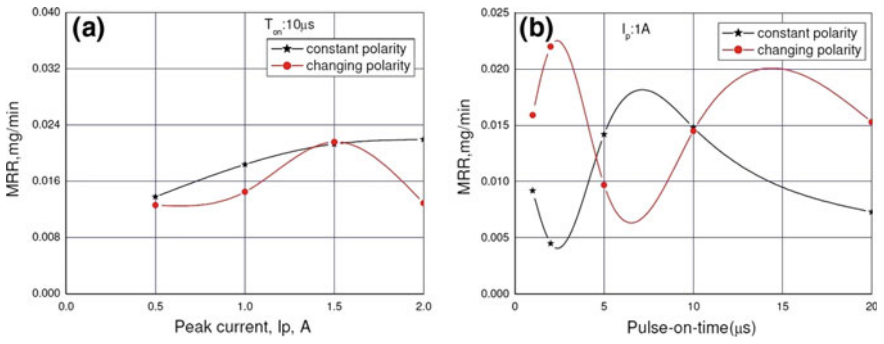

Fig. 3.36 Variation of MRR with **a** peak current and **b** pulse-on-time [59]

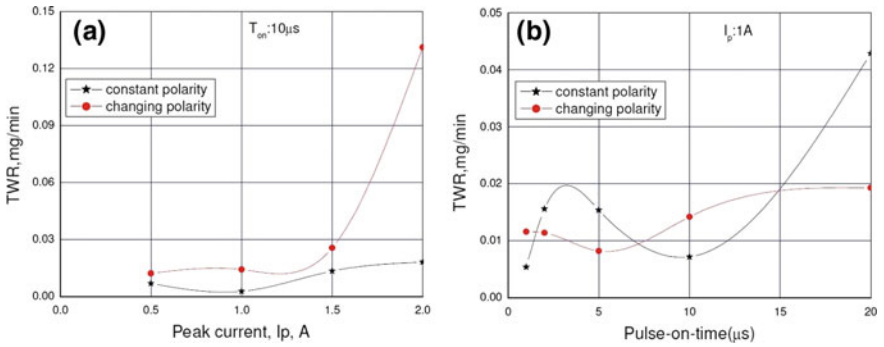

Fig. 3.37 Variation of TWR with **a** peak current and **b** pulse-on-time [59]

from 5 to 10 μs, MRR increases gradually in both cases. Furthermore, in the pulse-on-time range of 10–20 μs, MRR increases slowly for constant polarity whereas it decreases for changing polarity. It can also be observed that maximum MRR is obtained at the lower range of pulse-on-time, i.e. 1–5 μs. In the case of the changing polarity approach to machining, owing to change in polarity, the position of maximum liberation of heat energy due to sparking is changed and at the same time the number of sparking per cycle is increased for lower pulse-on-time. Thus the total heat energy generated in the discharge phenomenon is increased during the parametric setting and a high MRR is obtained.

Figure 3.37a, b show the variation of TWR with peak current and pulse-on-time respectively. It is observed from Fig. 3.37a, as expected, that TWR increases proportionally with the increase in peak current from 0.5 to 2 A at fixed pulse-on-time of 10 μs in both constant and changing polarity. The increase in TWR with the increase in peak current is due to the increase in discharge energy. The increase in magnitude of discharge energy rapidly deteriorates the tool geometry as the thermal energy is concentrated in a very small area (the size of the electrode in this case). However, it can be seen from Fig. 3.37a that TWR is greater with changing polarity; this is exactly opposite to the expectation outlined above, where it was thought that tool wear should be less in this case. This might have occurred owing to the removal of carbon deposition from the tool during normal polarity. However, when pulse-on-time was varied keeping peak current, duty factor, and flushing pressure constant as shown in Fig. 3.37b, TWR has decreased significantly with changing polarity in comparison to constant polarity. This indicates that pulse-on-time is the more critical factor in tool wear than peak current. Therefore, for minimum TWR it is better to use changing polarity with smaller pulse-on-time (1–10 μs) and low peak current of 1 A as this yields higher MRR and low TWR. This observation reveals that shorter pulse-on-time, which means a higher frequency of sparking, and low peak current are suitable for micro-EDM.

Figure 3.38a, b show the variation of OC with peak current and pulse-on-time, respectively. It is observed from Fig. 3.38a that OC decreases sharply from 0.5 to 1 A for both constant and changing polarity and thereafter increases monotonically

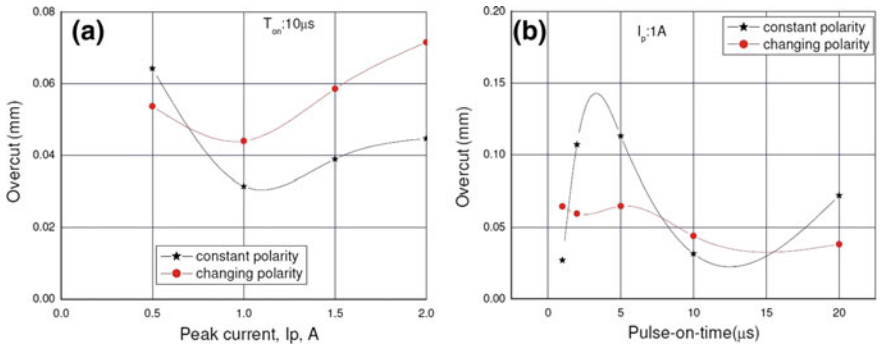

Fig. 3.38 Variation of OC with **a** peak current and **b** pulse-on-time [59]

with increasing peak current in both machining conditions. This clearly indicates that the optimum peak current setting is 1 A at the present level of process parameters range. If peak current is low, the discharge energy is also low, which means a longer machining time exposing the sidewall of the hole to secondary sparking resulting in larger OC. However, the increase in OC at higher peak current is due to higher discharge energy and larger debris concentration in the gap because of higher MRR. Also, it can be observed from Fig. 3.38b that OC increases steeply from 1 to 5 μs, decreases sharply from 5 to 10 μs, and again increases at 10–20 μs for constant polarity. Thus the OC fluctuates with the change in pulse-on-time for constant polarity. However, for changing polarity, OC is found to decrease gradually for pulse-on-time from 1 to 20 μs, thereby suggesting the benefit of using the changing polarity technique for achieving lower overcut in the machining of micro-holes, hence increasing the geometrical accuracy of the machined micro-hole in Ti–6Al–4V material. Further, it is observed throughout the range of pulse-on-time from 1 to 20 μs that the magnitude of OC is far lower with changing polarity than with constant polarity, which is an indicator in itself that changing polarity yields low OC and results in improvement of micro-hole geometry. This is due to the fact that the carbon particles, which are the by-product of the micro-EDM process, are deposited on the surface of the tool electrode and this helps in preventing secondary sparking. Thus only the end face or bottom face is exposed for sparking, thereby reducing OC and resulting in straight-through micro-hole generation, thus improving the accuracy of micro-hole machining.

It is observed from Fig. 3.39a, b that DVEE decreases sharply with the increase in peak current and pulse-on-time. The lowest DVEE is found at 1 A and 10 μs, which can be seen in the figures for both constant and changing polarity machining conditions. Also it is observed that DVEE is less with changing polarity than with constant polarity throughout the peak current and pulse-on-time ranges considered in the experiments. It can be concluded that with the novel polarity changing technique, a straight micro-hole is possible. As the depth of the micro-hole increases, the sparking points shift radially inward. When the polarity is changed the pointed tip of the micro-tool wears off uniformly, making the tool end broader and helping in machining a straight micro-hole, resulting in the decrease in DVEE.

Optical micrographs of the micro-holes (entry and exit diameter) machined with constant and changing polarity at 1 A/20 µs/95% duty factor/0.5 kgf/cm^2 are shown in Fig. 3.40a, b, respectively. The DVEE at parametric combination of 1 A/10 µs/95% duty factor/0.5 kg cm^{-2} for the constant polarity machining condition is 0.0270 mm, and for changing polarity the value is 0.0173 mm.

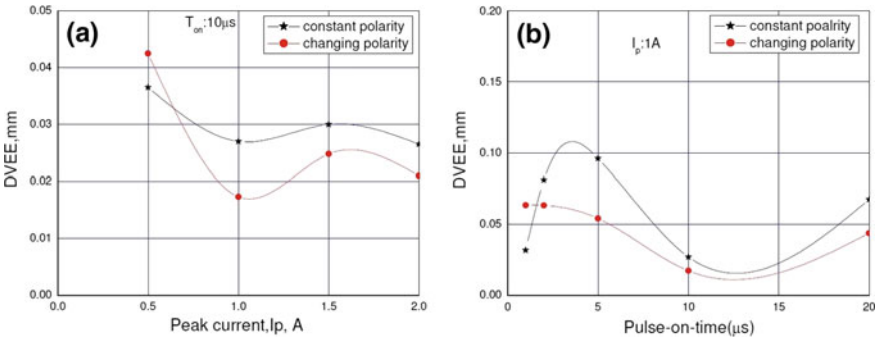

Fig. 3.39 Variation of DVEE with **a** peak current and **b** pulse-on-time [59]

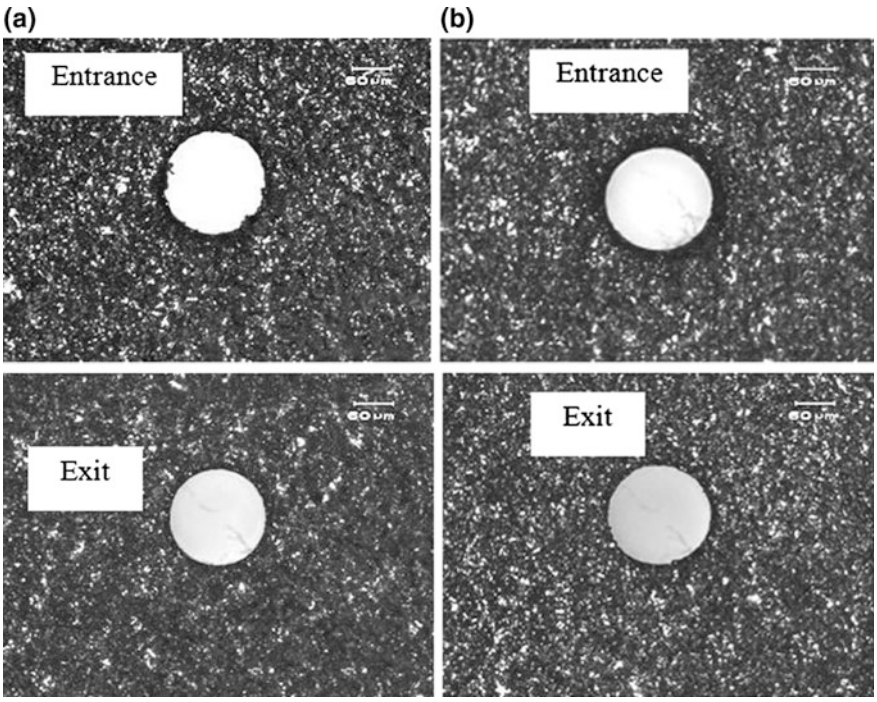

Fig. 3.40 Optical micrographs of micro-holes with **a** constant and **b** changing polarity machined at 1 A/20 µs/95% duty factor/0.5 kgf/cm^2

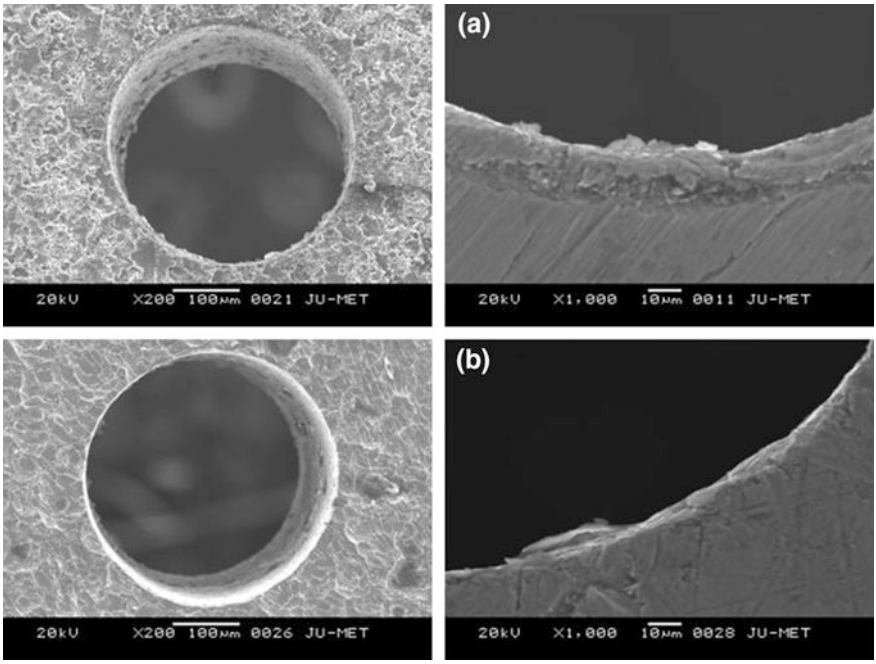

Fig. 3.41 SEM micrographs of micro-holes with **a** constant and **b** changing polarity machined at 1 A/20 µs/95% duty factor/0.5 kgf/cm^2

The comparison of these data and the micrographs clearly indicate that DVEE and geometrical shape are better when using the changing polarity condition for the micromachining of micro-holes by the micro-EDM. The SEM micrographs of machined micro-holes at parametric settings of 1 A/20 µs/95% duty factor/0.5 kg cm^{-2} with constant and changing polarity techniques are shown in Fig. 3.41a, b, respectively. It can be observed from these figures that the thickness of recast layer formed on micro-hole surface with polarity changing technique machining condition is less as compared to constant polarity machining condition corroborating the fact that the surface quality of the machined micro-hole has improved with this new machining technique. This observation clearly indicates that with changing polarity technique, a better machining condition is achieved during micro-hole machining by micro-EDM process.

3.11 Conclusions

In this chapter, a brief introduction of micro-EDM process and the implementation of innovative machining strategies for improving the process performances during machining was presented. Moreover, the principle of normal EDM and then

micro-EDM were described with brief details of sub-systems and significant process parameters with performance measures. Detailed research and investigation was performed during micro-EDM of Ti–6Al–4V alloy implementing various machining strategies such as ultrasonic vibration assisted micro-EDM, parametric influence and comparative study of process criteria employing two different dielectrics i.e. kerosene and de-ionized water, use of boron carbide mixed kerosene and de-ionized water as dielectrics, providing rotation of micro-tool electrode during micro-hole generation and reversing the polarity of electrodes. The experimental results show that these innovative machining strategies have great influences for improving the machining rate and geometrical accuracy in terms of material removal rate, tool wear rate, overcut and diameteral variance of entry and exit of micro-hole. Furthermore, the process performances also greatly depend on significant process parameters such as peak current, pulse-on-time and flushing pressure. As micro-EDM process is slow process, therefore, novel machining strategies mentioned above must be implemented to improve the process performances to improve the accuracy of micro-structure, surface finish and efficiency. Furthermore, innovative hybrid micro-machining processes can also be developed for micro-EDM to machine hard-to-machine materials like Ti–6Al–4V alloy for increasing the yield of micro-manufacturing.

Acknowledgements The authors acknowledge the financial support and assistance provided by CAS Ph-IV programme of Production Engineering Department of Jadavpur University under University Grants Commission (UGC), New Delhi, India.

References

1. Masuzawa T (2000) State of the Art of Micromachining. Annals of the CIRP 49(2):473-488
2. Ho KH, Newman ST (2003) State of the art electrical discharge machining (EDM). International Journal of Machine Tools & Manufacture 43(13):1287-1300
3. Kunieda M, Lauwers B, Rajurkar KP, Schumacher BM (2005) Advancing EDM through Fundamental Insight into the Process. CIRP Annals - Manufacturing Technology 54(2):64–87
4. König W, Klocke F (1997) Fertigungsverfahren - 3: Abtragen Und Generieren, Vol.3. Springer, Berlin
5. Pham DT, Dimov S, Bigot S, Ivanov A, Popov KB (2004) Micro-EDM—recent developments and research issues. Journal of Materials Processing Technology 149(1–3): 50–57
6. Gentili E, Tabaglio L, Aggogeri F (2005), Review on micromachining techniques. Courses Lectures, CISM International Centre for Mechanical Science 486:387-396
7. Katz Z, Tibbles CJ (2005) Analysis of Micro-scale EDM process. International Journal of Advanced Manufacturing Technology 25(9):923-928
8. Rajurkar KP, Levy G, Malshe A, Sundaram MM, McGeough J, Hu X, Resnick R, DeSilva A (2006) Micro and nano machining by electro-physical and chemical processes. Annals of the CIRP 55(2):643–666
9. Masuzawa T, Sata T, Kinoshita N (1971) The occurring mechanism of the continuous arc in micro-energy EDM by RC circuit. Journal of Japan Society of Electrical-Machining Engineers 5(9):35–52

10. Han F, Yamada Y, Kawakami T, Kunieda M (2004) Improvement of Machining Characteristics of Micro-EDM Using Transistor Type Isopulse Generator and Servo Feed Control. Precision Engineering 28(4):378–385
11. Masuzawa T, Fujino M (1980) Micro Pulse for EDM. In: Proceedings of the Japan Society for Precision Engineering Autumn Conference, Japan 140-142 (in Japanese)
12. Han F, Yamada Y, Kawakami T, Kunieda M (2003) Investigations on Feasibility of Sub Micrometer Order Manufacturing Using Micro-EDM. In: Proceedings of American Society of Precision Engineering (ASPE) Annual Meeting 30:551–554
13. Jahan MP, Wong YS, Rahman M (2009) A Study on the Fine-Finish Die-Sinking Micro-EDM of Tungsten Carbide Using Different Electrode Materials. Journal of Materials Processing Technology 209(8):3956–3967
14. Mahardika M, Tsujimoto T, Mitsui K (2008) A New Approach on the Determination of Ease of Machining by EDM Processes. International Journal of Machine Tools & Manufacture 48 (7-8):746–760
15. Yan BH, Huang FY, Chow HM, Tsai JY (1999) Micro-Hole Machining of Carbide by Electrical Discharge Machining. Journal of Materials Processing Technology 87(1-3):139–145
16. Hung JC, Lin JK, Yan BH, Liu HS, Ho PH (2006) Using a Helical Micro-Tool in Micro-EDM Combined with Ultrasonic Vibration for Micro-Hole Machining. Journal of Micromechanics and Microengineering 16(12):2705–2713
17. Levy GN, Ferroni B (1975) Planetary Spark Erosion - Applications and Optimization. In: Proceedings of the 16th MTDR Conference 291–297
18. Jahan MP, Rahman M, Wong YS (2011) Study on the Nano-Powder Mixed Sinking and Milling Micro-EDM of WC–Co. International Journal of Advanced Manufacturing Technology 53(1):167–180
19. Tsai YY, Masuzawa T (2004) An index to evaluate the wear resistance of the electrode in micro-EDM. Journal of Materials Processing Technology 149(1-3):304–309
20. Kunieda M, Lauwers B, Rajurkar KP, Schumacher BM (2005) Advancing EDM through Fundamental Insight into the Process. Annals of the CIRP 54(2):599–622
21. Yu Z, Jun T, Kunieda M (2004) Dry EDM of Cemented Carbide. Journal of Materials Processing Technology 149(1-3):353–357
22. Tao J, Shih AJ, Ni J (2008) Near-Dry EDM Milling of Mirror-Like Surface Finish. International Journal of Electrical Machining 13:29–33
23. Egashira K, Taniguchi T, Hanajima S (2006) Planetary EDM of Micro Holes. International Journal of Electrical Machining 11:15–18
24. Pradhan BB, Masanta M, Sarkar BR, Bhattacharyya B (2009) Investigation of electro-discharge micro-machining of titanium super alloy. International Journal of Advanced Manufacturing Technology 41:1094-1106
25. Pradhan BB, Bhattacharyya B (2009) Modelling of micro-electro discharge machining during machining of titanium alloy Ti-6Al-4V using response surface methodology and artificial neural network algorithm. Proceedings of the Institution of Mechanical Engineers Part B: Journal of Engineering Manufacture 223(6):683–693
26. Ali MY, Rahman NABA, Aris EBM (2012) Powder mixed micro electro discharge milling of titanium alloy: investigation of material removal rate. Advanced Materials Research 383–390:1759–1763
27. Meena VK, Azad MS (2012) Grey Relational Analysis of Micro-EDM Machining of Ti-6Al-4V Alloy. Materials and Manufacturing Processes 27(9):973-977
28. Porwal RK, Yadava V, Ramkumar J (2014) Modelling and multi-response optimization of hole sinking electrical discharge micromachining of titanium alloy thin sheet. Journal of Mechanical Science and Technology 28(2):653-661
29. Tiwary AP, Pradhan BB, Bhattacharyya B (2014) Application of multi-criteria decision making methods for selection of micro-EDM process parameters. Advances in Manufacturing 2(3):251-258

30. Kuriachen B, Mathew J (2014) Modeling of material removal mechanism in micro electric discharge milling of Ti-6Al-4V. Applied Mechanics and Materials 592–594:516–520
31. Plazaa S, Sancheza JA, Pereza E, Gila R, Izquierdob B, Ortegaa N, Pombob I (2014) Experimental study on micro EDM-drilling of Ti6Al4V using helical electrode. Precision Engineering 38(4):821–827
32. Moses MD, Jahan MP (2015) Micro-EDM machinability of difficult-to-cut Ti-6Al-4V against soft brass. International Journal of Advanced Manufacturing Technology 81(5):1345-1361
33. Tiwary AP, Pradhan BB, Bhattacharyya B (2015) Study on the influence of micro-EDM process parameters during machining of Ti–6Al–4V superalloy. International Journal of Advanced Manufacturing Technology 76(1–4):151–160
34. Kuriachen B, Mathew J (2016) Effect of powder mixed dielectric on material removal and surface modification in micro electric discharge machining of Ti-6Al-4V. Materials and Manufacturing Processes 31(4):439-446
35. Kuriachen B, Varghese A, Somashekhar KP, Panda S, Mathew J (2015) Three-dimensional numerical simulation of microelectric discharge machining of Ti-6Al-4V. International Journal of Advanced Manufacturing Technology 79(1):147-160
36. Kuriachen B, Mathew J (2016) Spark radius modeling of resistance-capacitance pulse discharge in micro-electric discharge machining of Ti-6Al-4V: an experimental study. International Journal of Advanced Manufacturing Technology 85(9):1983-1993
37. Kremer D, Lebrun JL, Hosari B, Moisan A (1989) Effects of ultrasonic vibrations on the performance in EDM. Annals of the CIRP 38(1):199–202
38. Ichikawa T, Natsu W (2013) Realization of micro-EDM under ultra-small discharge energy by applying ultrasonic vibration to machining fluid. The Seventeenth CIRP Conference on Electro Physical and Chemical Machining (ISEM) 6:326-331
39. Liew PJ, Yan J, Kuriyagawa T (2014) Fabrication of deep micro-holes in reaction-bonded SiC by ultrasonic cavitation assisted micro- EDM. International Journal of Machine Tools & Manufacture 76:13-20
40. Jahan MP, Rahman M, Wong YS, Fuhua L (2010) On-machine fabrication of high-aspect-ratio micro-electrodes and application in vibration-assisted micro-electro discharge drilling of tungsten carbide. Proceedings of the Institution of Mechanical Engineers Part B: Journal of Engineering Manufacture 224(5):795-814
41. Changshui G, Zhengxun L (2003) A study of ultrasonically aided micro-electrical-discharge machining by the application of work piece vibration. Journal of Materials Processing Technology 139(1-3):226-228
42. Prihandana GS, Mahardika M, Hamdi M, Wong YS, Mitsui K (2009) Effect of micro-powder suspension and ultrasonic vibration of dielectric fluid in micro-EDM processes-Taguchi approach. International Journal of Machine Tools & Manufacture 49(12-13):1035-1041
43. Ghoreishi M, Atkinson J (2002) A comparative experimental study of machining characterstics in vibratory, rotary and vibro-rotary electro- discharge machining. Journal of Materials Processing Technology 120(1-3):374-384
44. Shabgard MR, Sadizadeh B, Kakoulvand H (2009) The Effect of Ultrasonic Vibration of Workpiece in Electrical Discharge Machining of AISIH13 Tool Steel. International Journal of Mechanical, Aerospace, Industrial, Mechatronic and Manufacturing Engineering 3 (4):404-408
45. Garn R, Schubert A, Zeidler H (2011) Analysis of the effect of vibrations on the micro-EDM process at the workpiece surface. Journal of Precision Engineering 35(2):364-368
46. Tong H, Li Y, Wang Y (2008) Experimental research on vibration assisted EDM of micro-structures with non-circular cross-section. Journal of Materials Processing Technology 208(1-3):289–298
47. Zhang QH, Zhang JH, Deng JX (2002) Ultrasonic vibration electrical discharge machining in gas. Journal of Materials Processing Technology 129(1-3):135–138
48. Kim DJ, Yi SM, Lee YS, Chu CN (2006) Straight hole micro EDM with a cylindrical tool using a variable capacitance method accompanied by ultrasonic vibration. Journal of Micromechanics and Microengineering 16(5):1092–1097

49. Zhang QH, Du R, Zhang JH, Zhang QB (2006) An investigation of ultrasonic-assisted electrical discharge machining in gas. International Journal of Machine Tools & Manufacture 46(12-13):1582–1588
50. Bhattacharyya B, Gangopadhyay S, Sarkar BR (2007) Modelling and analysis of EDMed job surface integrity. Journal of Materials Processing Technology 189(1-3):169-177
51. Kibria G, Sarkar BR, Pradhan BB, Bhattacharyya B (2010) Comparative study of different dielectrics for micro-EDM performance during microhole machining of Ti-6Al-4V alloy. International Journal of Advanced Manufacturing Technology 48(5-8):557-570
52. Luo YF (1997) The dependence of interspace discharge transitivity upon the gap debris in precision electro-discharge machining. Journal of Materials Processing Technology 68 (2):127–131
53. Jeswani ML (1981) Effect of the addition of graphite powder to kerosene used as the dielectric fluid in electrical discharge machining. Wear 70(2):133–139
54. Pierson HO (1996) Handbook of Refractory Carbides and Nitrides: Properties, Characteristics, Processing and Applications, Noyes Publications, Westwood, New Jersey, USA
55. Luis CJ, Puertas I (2007) Methodology for developing technological tables used in EDM processes of conductive ceramics. Journal of Materials Processing Technology 189 (1-3):301-309
56. Ming QY, He LY (1995) Powder-suspension dielectric fluid for EDM. Journal of Materials Processing Technology 52(1):44–54
57. Tzeng YF, Lee CY (2001) Effects of powder characteristics on electro discharge machining efficiency. International Journal of Advanced Manufacturing Technology 17(8):586–592
58. Pradhan BB, Sarkar BR, Kibria G, Bhattacharyya B (2009) EDM with rotational electrode for machining micro holes in Ti-6Al-4V. Journal of Institution of Engineers (India) 89:3-8
59. Pradhan BB, Bhattacharyya B (2008) Improvement in microhole machining accuracy by polarity changing technique for microelectrode discharge machining on Ti–6Al–4V. Proceedings of the Institution of Mechanical Engineers Part B: Journal of Engineering Manufacture 222(2):163-173